Transverse dynamics of hard partons in nuclear media
and the QCD dipole

Urs Achim Wiedemann

Theory Division, CERN, CH-1211 Geneva 23, Switzerland

(March 13, 2000)

We derive the non-abelian generalization of the Furry approximation which describes the transverse dynamical evolution of a hard projectile parton inside a spatially extended colour target field. This provides a unified starting point for the target rest frame description of the nuclear dependence of a large class of observables. For the case of the virtual $\gamma^* \to q\bar{q}$ photoabsorption cross section, we investigate then in detail under which conditions the nuclear dependence encoded in the Furry wavefunctions can be parametrized by a $q\bar{q}$ QCD dipole cross section. The important condition is colour triviality, i.e., the property that for arbitrary N-fold rescattering contributions the only non-vanishing colour trace is $N_c C_F^N$. We give proofs for the colour triviality of the inelastic, diffractive and total photoabsorption cross section measured inclusively or with one jet resolved in the final state. Also, we list examples for which colour interference effects remain. Colour triviality allows us to write the DIS nuclear structure function F_2 for small Bjorken $x_{\rm Bj}$ in terms of a path integral which describes the transverse size evolution of the $q\bar{q}$ pair in the nuclear colour field. This expression reduces in an opacity expansion to the $N = 1$ result of Nikolaev and Zakharov, and in the eikonal approximation to the Glauber-type rescattering formulas first derived by Mueller. In the harmonic oscillator approximation of the path integral, we quantify deviations from the eikonal limit. Their onset is characterized by the scales L/l_f and $E_\perp^{\rm tot} L$ which relate the longitudinal extension L of the nuclear target to the coherence length l_f and the total transverse energy $E_\perp^{\rm tot}$ accumulated by the q-$\bar{q}$-pair.

I. INTRODUCTION

The partonic interpretation of physical processes and their nuclear dependence is Lorentz frame dependent. Drell-Yan, e.g., is a q-$\bar{q} \to \gamma^*$-fusion in the infinite momentum frame, but it becomes a γ^*-bremsstrahlung radiation off the projectile quark if viewed in the target rest frame [1,2]. Similarly, nuclear shadowing is due to the recombination of partons from different nucleons, if viewed in the infinite momentum frame [3]. In the target frame, it arises from non-additive contributions of the rescattering of the hadronic γ^*-Fock states in a spatially extended medium [4-8]. The descriptions in different Lorentz frames are equivalent, of course. But depending on the physical problem at hand, a well-chosen Lorentz frame may provide a particularly simple partonic interpretation. To study the nuclear dependence of physical processes, the target rest frame provides arguably the most intuitive picture. QCD factorization theorems can be expected to hold for the nuclear dependence of high-p_t processes only [9-11], and thus a large variety of other approaches to the nuclear dependence of hard processes exists in the literature [1,5,12-24]. These exploit that in the target rest frame, the nuclear dependence of a physical process P with transition amplitude $\langle \Psi_i | P | \Psi_f \rangle$ can be attributed often to the multiple rescattering of the hard in- and outgoing partons inside the soft spatially extended target colour field. In the simplest cases, this rescattering effect can be described by multiplying the free in- and outgoing wavefunctions with straight eikonal Wilson lines which account for the leading medium-induced colour rotation of projectile quarks [1,25].

In the present work, we derive and study a more refined approximation scheme for in- and outgoing wavefunctions Ψ_i and Ψ_f which includes the leading transverse dynamical evolution of the projectile partons inside the target. To this end, we derive in section II explicit expressions for Ψ_i and Ψ_f which approximate to leading order $1/E$ in the norm *and* next to leading order in the phase the solution of the Dirac equation in the presence of a spatially extended colour field. The $1/E$-corrections included in these solutions are known to provide the leading contribution for observables which are essentially determined by the destructive interference between different production amplitudes as, e.g., the non-abelian Landau-Pomeranchuk-Migdal (LPM) effect [12-21] or the nuclear dependence of Drell-Yan pair production [2,20]. Indeed, our derivation of Ψ_i and Ψ_f draws on exactly the same approximation schemes which were used in recent studies [12,26] of the nuclear dependence of these observables. In section II, however, we discuss this rescattering effect without reference to a particular observable. In this way, we obtain a compact expression which turns out to be the non-abelian generalization of the abelian Furry approximation [20,21] and which may serve as building block in the calculation of very different nuclear dependencies.

The main technical complication in working with non-abelian Furry wavefunctions is that they involve a path-integral over a path-ordered non-abelian Wilson line. In section III and IV, we show for the example of the $\gamma^* \to q\bar{q}$ photodissociation process how explicit and exact calculations can be done despite this complication. The key step is a diagrammatic technique first used by

Mueller and collaborators [4,15-18,27] which allows to establish the colour triviality of certain cross sections involving N-fold rescattering processes. Here, colour triviality means that the contribution to a medium-dependent observable to N-th order in the opacity involves only colour traces which reduce to the N-th power of the Casimir. This renders the problem essentially abelian. In section IV C, we derive the corresponding diagrammatic identities for our configuration space formulation of partonic rescattering. We then use these identities in explicit proofs of the colour triviality of the inelastic and diffractive part of the inclusive and one-fold differential (i.e. one jet resolved) photoabsorption cross section. At least for the $\gamma^* \to q\bar{q}$ photodissociation cross section, all colour trivial observables turn out to be given in terms of the transverse dynamical evolution of a QCD dipole which is described by a simple path integral $\mathcal{K}$. We discuss the eikonal limit in which the transverse dynamical evolution is neglected, and we quantify the leading corrections to this limiting case.

We choose for all explicit calculations the photodissociation process $\gamma^* \to q\bar{q}$ mainly since it is the simplest example which allows to illustrate all technical difficulties associated with the non-abelian Furry approximation and colour interference effects. One may ask to what extent the same approach can be applied to other or more exclusive observables or to other models of the medium. Two aspects of this very general question are addressed here: Firstly, we give in section IV B and IV E examples of (more exclusive) photoabsorption processes which are not colour trivial, thus indicating the limitations of the approach advocated here. Secondly, we argue in section V that the specific model ansatz for in-medium rescattering is not instrumental for our results. We do believe that the compact configuration-space notation used throughout this work will prove an important tool in establishing and exploiting the colour triviality of various other observables which show interesting nuclear dependencies. This, however, lies outside the scope of the present work. In the Conclusions, we summarize our main results and we shortly comment an these further perspectives.

II. ASYMPTOTIC WAVEFUNCTIONS FOR RESCATTERING PARTICLES

We want to calculate the nuclear dependence of some physical process P with transition amplitude $\langle \Psi_i | P | \Psi_f \rangle$ by describing how the medium affects the propagation of the in- and outgoing wavefunctions Ψ_i, Ψ_f. For the case of the photodissociation process $\gamma^* \to q\bar{q}$ depicted in Fig. 1a this means that we write the corresponding transition amplitude in the form

$$\langle \Psi_i | P | \Psi_f \rangle = ie \int d^4x \, \Psi_u^\dagger(x, p_1) \, \gamma^0$$

$$\times \epsilon_\mu \, \gamma^\mu \, e^{i\,k \cdot x} \, \Psi_v(x, p_2) \, . \quad (2.1)$$

Here, the physical process P is determined by the photon-quark vertex $ie\epsilon \cdot \gamma \, e^{ikx}$. In this section, we derive explicit expressions for the medium-dependence of these asymptotic wavefunctions irrespective of a particular process. Section II A explains the solution of the corresponding abelian problem, section II B establishes the non-abelian extension. In the remaining sections of this paper, we shall discuss then for the example of the photodissociation (2.1) how explicit calculations can be done.
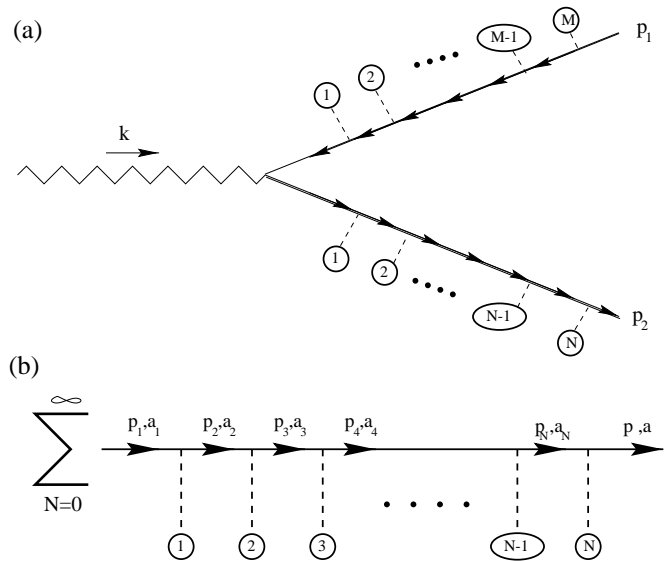

FIG. 1. (a) Contribution to the photodissociation process $\gamma^* \to q\bar{q}$ with N- and M-fold final state rescattering for the outgoing quark and antiquark. (b) Sum over rescattering diagrams for an outgoing antiquark which leaves the production vertex with momentum p_1 and colour a_1. To leading order in opacity, this resums all rescattering effects and defines the non-abelian Furry wavefunction (2.12).

A. Abelian Furry approximation

We consider a relativistic positron with momentum $(E_2, \mathbf{p}_2)$ $(E_2 \gg m)$. Prior to its detection, this positron undergoes multiple small-angle scattering in a spatially extended medium, described e.g. by a collection $U(\mathbf{x})$ of single scattering potentials $\varphi_i(\mathbf{x}) = \varphi(\mathbf{x} - \check{\mathbf{x}}_i)$ localized at spatial positions $\check{\mathbf{x}}_i$,

$$U(\mathbf{x}) = \sum_{i=1}^{\infty} \varphi(\mathbf{x} - \check{\mathbf{x}}_i) \, . \quad (2.2)$$

The asymptotic electron wavefunction Ψ is a solution to the Dirac equation in this spatially extended field:

$$\left[i \frac{\partial}{\partial t} - U(\mathbf{x}) - m \, \gamma_0 + i \, \boldsymbol{\alpha} \cdot \boldsymbol{\nabla} \right] \Psi(x, p_2) = 0 \, . \quad (2.3)$$

2

Which approximation for $\Psi(x, p_2)$ keeps the leading medium-dependence ? An expansion of Ψ in powers of the coupling constant does not since it amounts to an expansion in powers of the single scattering potential φ rather than containing the leading order effect of U. In QED, the leading U-dependence is kept in the Furry approximation [20,21] which is a high energy expansion of the solution of the Dirac equation. For the outgoing positron wavefunction, it reads

$$\Psi_F(x, p_2) = e^{iE_2 t - ip_2 z} \hat{D}_2 F(\mathbf{x}, \mathbf{p}_2) v(\mathbf{p}_2). \qquad (2.4)$$

which is exact to order $O(U/E)$ and $O(1/E^2)$. Here, $\hat{D}_i$ denotes a differential operator

$$\hat{D}_i = 1 - i\frac{\boldsymbol{\alpha} \cdot \boldsymbol{\nabla}}{2\, E_i} - \frac{\boldsymbol{\alpha} \cdot (\mathbf{p}_i - \mathbf{n}\, p_i)}{2\, E_i},$$
$$\boldsymbol{\alpha} = \gamma_0 \boldsymbol{\gamma} \quad ; \quad z = \boldsymbol{n} \cdot \boldsymbol{x} \quad ; \quad p_i = |\boldsymbol{p}_i|, \qquad (2.5)$$

and the unit vector $\boldsymbol{n}$ specifies the *longitudinal* direction. The differential operator acts on the transverse wavefunctions F. For very late times, i.e., for far forward longitudinal distances x_L, this wavefunction satisfies plane wave boundary conditions

$$F(\mathbf{x}_\perp, x_L, \mathbf{p}_2) = \exp\left\{ -i\, \mathbf{p}_2^\perp \cdot \mathbf{x}_\perp + i\, \frac{\mathbf{p}_2^{\perp\, 2}}{2\, p_2} x_L \right\}, \qquad (2.6)$$

$$F(\mathbf{y}_\perp, y_L, \mathbf{p}_2) = \int d\mathbf{x}_\perp\, G(\mathbf{x}_\perp, x_L; \mathbf{y}_\perp, y_L | p_2)$$
$$\times F(\mathbf{x}_\perp, x_L, \mathbf{p}_2). \qquad (2.7)$$

Its evolution to finite longitudinal distances is determined by the retarded Green's function G whose path integral representation reads

$$G(z', \boldsymbol{r}'; z, \boldsymbol{r}\,|\, p) =$$
$$\int \mathcal{D}\boldsymbol{r}(\xi) \exp\left\{ \int\limits_z^{z'} d\xi \left[\frac{ip}{2} \dot{\mathbf{r}}^2(\xi) - i\, U\big(\mathbf{r}(\xi), \xi\big) \right] \right\}. \qquad (2.8)$$

Here, $\dot{r} = dr/d\xi$ and G satisfies the boundary conditions $\mathbf{r}(z) = \mathbf{r}$, $\mathbf{r}(z') = \mathbf{r}'$, with $G(z' = z, \mathbf{r}'; z, \mathbf{r}|p) = \delta(\mathbf{r}' - \mathbf{r})$, and $G(z', \boldsymbol{r}'; z, \boldsymbol{r}\,|\, p) = 0$ for $z > z'$. The Green's function (2.8) describes the Brownian motion of the projectile particle in the plane transverse to the beam. This is the leading medium effect on the propagation of the projectile. Starting from the abelian Furry wavefunction (2.4), the KST-formalism [20,21] then allows to describe e.g. the medium dependence of the LPM-bremsstrahlung spectrum [20,21]. One of the main motivations for what follows is the question to what extent the application of the same approach to non-abelian problems is justified.

B. Non-abelian Furry approximation

To find the non-abelian generalization of the Furry approximation, we consider a spatially extended static colour potential of the form

$$A_\mu(\mathbf{x}) = \delta_{0\mu} \sum_{i=1}^\infty \varphi_i^a(\mathbf{x})\, T^a, \qquad (2.9)$$

$$\varphi_i^a(\mathbf{x}) = \varphi(\mathbf{x} - \check{\mathbf{x}}_i)\, \delta^{a\, a_i}, \qquad (2.10)$$

where T^a, $(a = 1, \ldots, N_c^2 - 1)$, denote the generators of the $SU(N_c)$ colour representation of the projectile parton. The i-th scattering center is located at $\check{\mathbf{x}}_i$ and exchanges a specific colour charge $a = a_i$.

For the spatial support of the potentials φ_i^a we take the rapid fall-off of a Yukawa potential with some Debye screening mass M. We assume that the mean free path of the projectile parton in the medium is taken to be much larger than $1/M$. This ansatz for (2.10) is known as Gyulassy-Wang model [12,13] and was originally introduced to mimic rescattering effects of hard partons in the colour-deconfined matter created in the early phase of a relativistic heavy ion collisions.

To leading order $O(1/E)$, the Feynman diagram in Fig. 1b is the only α_s^N rescattering term. Rescattering contributions involving 3- or 4-gluon vertices are known to come with spatial suppression factors in the Gyulassy-Wang model [12,16]. The N-fold rescattering of a hard parton in the colour field (2.9) is thus determined by

$$I^{(N)}(\mathbf{y}) = e^{-i\mathbf{p}_1 \cdot \mathbf{y}} \mathcal{P} \left(\prod_{i=1}^N \int \frac{d^3\mathbf{p}_i}{(2\pi)^3}\, d^3\mathbf{x}_i\, \frac{i\,(\not{p}_i + m)\,\gamma_0}{p_i^2 - m^2 + i\,\epsilon} \right.$$
$$\left. \times [-i\, A_0(\mathbf{x}_i)]\, e^{-i\,\mathbf{x}_i \cdot (\mathbf{p}_{i+1} - \mathbf{p}_i)} \right) v^{(r)}(\mathbf{p}). \quad (2.11)$$

Here, the quark leaves some production vertex with momentum p_1 and colour a_1. It undergoes N gluon exchanges with the spatially extended colour potential A_μ, emerging in the "final state" with momentum p and colour a. $I^{(N)}(\mathbf{y})$ is a matrix in the colour representation of the projectile. The path-ordering $\mathcal{P}$ implies that $A_0(\mathbf{x}_{i+1})$ stands to the right of $A_0(\mathbf{x}_i)$. The diagram in Fig. 1 denotes the component $I_{a_1\, a}^{(N)}$ of this matrix. The momentum transfers to the quark line are written as Fourier transforms of the static scattering potential with respect to the relative momenta $\mathbf{p}_{i+1} - \mathbf{p}_i$. Finally, instead of an explicit production vertex, we have introduced in (2.11) the incoming plane wave $\exp[-i\, \mathbf{p}_1 \cdot \mathbf{y}]$. This factor allows to glue the above Feynman diagram via $\mathbf{y}$-integration onto another subprocesses P without specifying P at the present stage.

In appendix A, we approximate the norm of $I^{(N)}$ to leading order $O(1/E)$ and the phase to next to leading order. Summing then over contributions for arbitrarily many N rescatterings in the medium, we find the non-abelian Furry wavefunction

$$\Psi_v(y^0, \mathbf{y}, p) = e^{i\, E\, y^0} \sum_{N=0}^\infty I^{(N)}(\mathbf{y})$$
$$= e^{i\, E\, y^0 - i\, p\, y_L} \hat{D}\, F(\mathbf{y}, \mathbf{p})\, v^{(r)}(\mathbf{p}). \qquad (2.12)$$

3

This expression compares directly to the abelian Furry approximation (2.4). In (2.12), $\hat{D}$ is the operator (2.5) with $p_i = p$, and F is the outgoing transverse wavefunction evolved from its asymptotic plane wave form to $\mathbf{y}$ with the Green's function $\bar{G}$,

$$
\begin{aligned}
F(\mathbf{y}, \mathbf{p}) = \int d\mathbf{x}_\perp \, \bar{G}(\mathbf{y}_\perp, y_L; \mathbf{x}_\perp, x_L | p) \\
\times F(\mathbf{x}_\perp, x_L, \mathbf{p}) \,.
\end{aligned}
\tag{2.13}
$$

The Green's function $\bar{G}$ is the non-abelian generalization of the Green's function (2.8). It can be defined explicitly by its expansion in powers of the scattering potential A_0:

$$
\begin{aligned}
\bar{G}(\mathbf{r}, z; \mathbf{r}', z'|p) &\equiv \bar{G}_0(\mathbf{r}, z; \mathbf{r}', z'|p) - i \int\limits_z^{z'} d\xi \\
&\times \int d\boldsymbol{\rho} \, \bar{G}_0(\mathbf{r}, z; \boldsymbol{\rho}, \xi|p) \, A_0(\boldsymbol{\rho}, \xi) \, \bar{G}_0(\boldsymbol{\rho}, \xi; \mathbf{r}', z'|p) \\
&+ \mathcal{P} \int\limits_{z_L}^{x_L} d\xi_1 \int\limits_{\xi_1}^{x_L} d\xi_2 \int d\boldsymbol{\rho}_1 \, d\boldsymbol{\rho}_2 \, \bar{G}_0(\mathbf{r}, z; \boldsymbol{\rho}_1, \xi_1|p) \\
&\times i \, A_0(\boldsymbol{\rho}_1, \xi_1) \, \bar{G}_0(\boldsymbol{\rho}_1, \xi_1; \boldsymbol{\rho}_2, \xi_2|p) \\
&\times i \, A_0(\boldsymbol{\rho}_2, \xi_2) \, \bar{G}(\boldsymbol{\rho}_2, \xi_2; \mathbf{r}', z'|p) \,.
\end{aligned}
\tag{2.14}
$$

Here, $\bar{G}_0$ is the free non-interacting Green's function

$$
\bar{G}_0(\mathbf{r}, z; \mathbf{r}', z'|p) \equiv \frac{p}{2\pi i(z'-z)} \exp\left\{ \frac{ip\,(\mathbf{r} - \mathbf{r}')^2}{2(z'-z)} \right\} \,,
\tag{2.15}
$$

and the path ordering $\mathcal{P}$ in (2.14) ensures that the potential $A_0(\boldsymbol{\rho}_2, \xi_2)$ stands to the right of the potential $A_0(\boldsymbol{\rho}_1, \xi_1)$. In contrast to the retarded Green's function (2.8) which is only non-vanishing for $z' > z$, we shall use the Green's function $\bar{G}$ in (2.14) for $z' > z$ and $z > z'$ by defining

$$
\bar{G}(\mathbf{r}', z'; \mathbf{r}, z|p) \equiv \bar{G}^\dagger(\mathbf{r}, z; \mathbf{r}', z'|p) \,, \qquad \text{for } z' > z \,.
\tag{2.16}
$$

Note that for a hermitian scattering potential, this latter definition (2.16) is indeed compatible with the representation (2.14). Hermitian conjugation automatically inverts the path-ordering. A very compact notation for the expansion (2.14) can be given in terms of a path-ordered Wilson line $W([\mathbf{r}]; z, z')$ which follows the non-abelian potential A_0 from initial position $(\mathbf{r}(z), z)$ to final position $(\mathbf{r}(z'), z')$ along the path $\mathbf{r}(\xi)$

$$
\bar{G}(\mathbf{r}, z; \mathbf{r}', z'|p) =
$$
$$
= \int \mathcal{D}\boldsymbol{r}(\xi) \exp\left\{ \frac{ip}{2} \int\limits_z^{z'} d\xi \, \dot{\mathbf{r}}^2(\xi) \right\} W([\mathbf{r}]; z, z') \,,
\tag{2.17}
$$

$$
W([\mathbf{r}]; z, z') = \mathcal{P} \exp\left\{ -i \int\limits_z^{z'} d\xi \, A_0(\mathbf{r}(\xi), \xi) \right\} \,.
\tag{2.18}
$$

Again, operators at larger longitudinal distances ($z' > z$) stand to the right. Expanding the Wilson line to fixed order $O(A_0^n)$ coincides with the representation (2.14). The non-abelian Furry approximation thus differs from the abelian one essentially by path-ordering in the Green's function $\bar{G}$ which describes the dynamical evolution of the transverse wavefunction.

To obtain the result (2.12), it is crucial that we approximate first the N-fold rescattering diagram $I^{(N)}$, keeping the phase factor to order $O(1/E)$ and then resum contributions for arbitrary N. If one parallels the derivation of the abelian case by directly starting from the solution of the non-abelian Dirac equation in the presence of a spatially extended colour field, one arrives at the recursive solution of Buchmüller and Hebecker [28]. The starting point for their recursion formula is a straight eikonal Wilson line, and the recursion includes corrections to fixed order in energy. An explicit n-fold iterated expression is thus correct to fixed order $O(1/E^n)$, but it does not contain the $O(1/E)$-corrections to the *phase* of the wavefunction, which is characteristic for the Furry approximation. Our diagrammatic approach allows to keep this phase. For large but finite incident energy, our solution is thus characteristically different from that given in Ref. [28]. [We have checked, e.g., that the abelian version of [28] does not lead to the correct medium dependence of the QED bremsstrahlung spectrum while the abelian version of (2.12) does. This difference of both solutions is expected since the bremsstrahlung spectrum is sensitive to interference effects which stem from the $O(1/E)$-contributions to the phase of the wavefunctions [21].]

In the infinite energy limit, the solution (2.12) reduces to the straight eikonal Wilson line

$$
\lim_{\nu \to \infty} \bar{G}(\mathbf{r}, z; \mathbf{x}_\perp, x_L | \nu) = W([\mathbf{r}_s]; z, x_L) \,,
\tag{2.19}
$$

$$
\mathbf{r}_s(\xi) = \mathbf{x}_\perp \frac{\xi - z}{x_L - z} + \mathbf{r} \frac{x_L - \xi}{x_L - z} \,,
\tag{2.20}
$$

which is the leading order input for the recursion formula of Ref. [28]. This expression is often used to describe the leading colour rotation of the hard parton in a soft colour field [1,25].

The Furry wavefunction (2.12) derived here allows for the description of the nuclear dependence of a large class of physical observables. Before illustrating this for a specific example, let us comment shortly on the limitation of a description of nuclear dependencies in terms of $\langle \Psi_i | P | \Psi_f \rangle$. Strictly speaking, of course, QCD factorization theorems for observables including rescattering effects have been established (and can be expected to hold) only for processes for which kinematical constraints ensure extremely high transverse momentum transfers ($\gg \Lambda_{QCD}$), [9-11]. In this sense, the description of the *soft* nuclear rescattering of hard partons always depends on additional assumptions and different approaches may be taken [1,12,15]. In particular, we assume (as all other

4

treatments do) that the leading nuclear dependence can be obtained using the idealization of "asymptotic" parton wavefunctions, i.e., without considering parton fragmentation. Since parton fragmentation and soft parton rescattering involve transverse momenta of the same order, this is a requirement on the spatial separation of the two phenomena and amounts to an energy-dependent limit on the longitudinal extension L of the nuclear target up to which this description can be expected to apply. Moreover, the ad hoc separation of the transition amplitude into a production P and a final state wavefunction including rescattering effects may be oversimplified for specific processes. We think, e.g., of the production and rescattering of a heavy quarkonium state with specific quantum numbers. Taking P to be the production of the heavy q-$\bar{q}$-pair, it is not clear a priori to what extent final state rescattering modifies the quantum numbers of this state. First studies indicate [29] that the discussion of this problem requires a classification of the hardness of medium-induced momentum transfers which lies outside the scope of the present calculation. To sum up: the discussion of the nuclear dependence of hard observables in terms of $\langle \Psi_i | P | \Psi_f \rangle$ seems justified if no other soft scale (introduced e.g. by parton fragmentation or by the binding energy of the final state) interfers significantly with the final state rescattering effect described by the Furry wavefunctions. The non-abelian LPM-effect [12,13,15-18], the nuclear dependence of Drell-Yan yields [2,20] and nuclear shadowing [5,6] are prominent examples for which a description in terms of $\langle \Psi_i | P | \Psi_f \rangle$ seems suitable.

III. PHOTODISSOCIATION

In this section, we give a closed expression for the $\gamma^* \to q\bar{q}$ photodissociation cross section $\sigma^{\gamma^* \to q\bar{q}}$ in terms of the non-abelian Green's function $\bar{G}$ and the squared in-going wavefunction Φ of a freely evolving q-$\bar{q}$-pair. This photodissociation cross section contributes to the total virtual photoabsorption cross section $\sigma_{total}^{\gamma^*}$ which is related to the deep inelastic structure function F_2, [30]

$$F_2(x, Q^2) = \frac{Q^2}{4\pi^2\,\alpha_{\rm em}} \sigma_{total}^{\gamma^*}(x, Q^2)\,. \tag{3.1}$$

In the target rest frame, one can show that photodissociation as depicted in Fig. 2b dominates for small Bjorken x over the γ^*-q fusion process shown in Fig. 2a [6]. The leading corrections to $\sigma_{\rm total}^{\gamma^* \to q\bar{q}}$ come from initial state gluon radiation [6,32] which we neglect in what follows.

We consider a virtual photon of four momentum $k = (\nu, \mathbf{0}_\perp, \sqrt{\nu^2 + Q^2})$ which dissociates into a quark-antiquark pair in the time interval $-T/2 < t < T/2$. The dissociation cross section is

$$\sigma_{\rm total}^{\gamma^* \to q\bar{q}} = \frac{1}{2\,|k^L|\,T} \int dX\, |S_{fi}|^2\,, \tag{3.2}$$

where the phase space element is written in terms of the on-shell momenta of the outgoing quarks,

$$dX = \frac{d^3 p_1}{(2\pi)^3\, 2\,|E_1|} \frac{d^3 p_2}{(2\pi)^3\, 2\,|E_2|}\,. \tag{3.3}$$

The rescattering of these quarks in the spatially extended colour field is described by the Furry wavefunctions in the dissociation amplitude

$$S_{fi} \equiv S_{fi}^\mu\, \epsilon_\mu\,, \tag{3.4}$$

$$S_{fi}^\mu = ie \int d^4x\, \Psi_u^\dagger(x, p_1)\, \gamma^0\, \gamma^\mu$$
$$\times e^{-\epsilon\,|z|}\, e^{i\,k\cdot x}\, \Psi_v(x, p_2)\,. \tag{3.5}$$

To discuss the case of different photon polarizations, we write this disscociation amplitude as a contraction of S_{fi}^μ with the polarization vector ϵ_μ. To shorten our notation, we do not keep track of the fractional charge e_q of the quark and of the number of flavours. To do this, all our final results have to be supplemented by a sum over the available flavour channels weighted by e_q^2.
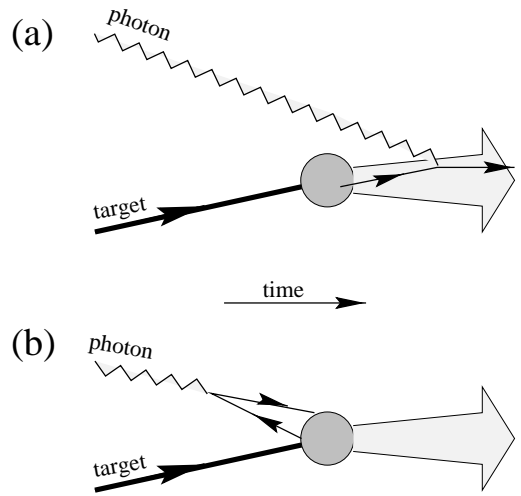
FIG. 2. Two possible time orderings for the interaction of a virtual photon with a nuclear target. At small Bjorken x, the $\gamma^* \to q\bar{q}$ photodissociation process (b) dominates over the γ^*-q-fusion, see Ref. [6].

Inserting the Furry wavefunctions for quark and antiquark, see (2.12), we can separate in (3.5) an energy conserving δ-function, $S_{fi}^\mu = ie\,(2\pi)\,\delta(E_2 - E_1 - \nu)\,M_{fi}^\mu$. We introduce the fraction α of the initial energy carried by one quark, $E_2 = \alpha\nu$, $E_1 = -(1-\alpha)\,\nu$. Here, E_1 is negative, since the corresponding 4-momentum p_1 flows into the quark-photon vertex, see Fig. 1a. After coordinate transformation $(p_1^L, p_2^L) \to (\alpha, k^L)$, the photodissociation cross section reads

$$\sigma_{\rm total}^{\gamma^* \to q\bar{q}} = \alpha_{\rm em} \int \frac{d\alpha}{4\,\nu^2\,\alpha\,(1-\alpha)}$$

5

$$\times \int \frac{d\mathbf{p}_1^\perp}{(2\pi)^2}\frac{d\mathbf{p}_2^\perp}{(2\pi)^2} \langle |M_{fi}|^2\rangle . \tag{3.6}$$

Here, we have used Fermi's golden rule and the k^L-integration to eliminate the two energy-conserving δ-functions. The brackets $\langle\ldots\rangle$ denote an in-medium average over the colour field A_μ which will be specified below. The probability $|M_{fi}|^2$ can be written in terms of the full interacting Green's functions (2.17) as

$$|M_{fi}|^2 = \int d^3\mathbf{y}\, d^3\bar{\mathbf{y}}\, e^{i\,q\,(y_L-\bar{y}_L)}\, e^{-\epsilon(|y_L|+|\bar{y}_L|)}\int d\mathbf{x}_\perp$$
$$\times d\mathbf{x'}^\perp\, d\bar{\mathbf{x}}_\perp\, d\bar{\mathbf{x}}'_\perp\, e^{i\,\mathbf{p}_1^\perp\cdot(\mathbf{x'}^\perp-\bar{\mathbf{x}}'_\perp)}\, e^{-i\,\mathbf{p}_2^\perp\cdot(\mathbf{x}_\perp-\bar{\mathbf{x}}_\perp)}$$
$$\times \bar{G}(\mathbf{x};\mathbf{y}|p_2)\,\epsilon_\mu \hat{\Gamma}^\mu\, \bar{G}(\mathbf{y};\mathbf{x'}|p_1)$$
$$\times \bar{G}(\bar{\mathbf{x}}';\bar{\mathbf{y}}|p_1)\,\epsilon_\nu \hat{\Gamma}^{*\nu}\, \bar{G}(\bar{\mathbf{y}};\bar{\mathbf{x}}|p_2) . \tag{3.7}$$

In general, all spatial coordinates can be different for M_{fi} and $M_{fi}^\dagger$. We characterize those for $M_{fi}^\dagger$ by a bar. The spinor structure of the Furry wavefunctions (2.12) is contained in (3.7) in the vertex function

$$\hat{\Gamma}^\mu = u^{(r')\dagger}(-p_1)\,\hat{D}_1^*\,\gamma^0\,\gamma^\mu\,\hat{D}_2\, v^{(r)}(p_2) . \tag{3.8}$$

In appendix B, we discuss how these vertex functions combine with free Green's functions $\bar{G}_0$ to the incoming q-$\bar{q}$ Fock state. In terms of the square $\Phi(\Delta\mathbf{z};\Delta\bar{\mathbf{z}};\alpha)$ of this Fock state, the differential photodissociation cross section (3.6) takes the form

$$\frac{\sigma_{\text{total}}^{\gamma^*\to q\bar{q}}}{d\alpha\, d\mathbf{p}_1^\perp\, d\mathbf{p}_2^\perp}$$
$$= \frac{\alpha_{\text{em}}}{(2\pi)^4}\int d\mathbf{b}_1\, d\mathbf{b}_2\, d\bar{\mathbf{b}}_1\, d\bar{\mathbf{b}}_2\, \Phi(\Delta\mathbf{b};\Delta\bar{\mathbf{b}};\alpha)$$
$$\times \int d\mathbf{x}_\perp\, d\mathbf{x'}_\perp\, d\bar{\mathbf{x}}_\perp\, d\bar{\mathbf{x}}'_\perp\, e^{i\,\mathbf{p}_1^\perp\cdot(\mathbf{x'}_\perp-\bar{\mathbf{x}}'_\perp)}\, e^{-i\,\mathbf{p}_2^\perp\cdot(\mathbf{x}_\perp-\bar{\mathbf{x}}_\perp)}$$
$$\times \Big\langle \bar{G}(\bar{\mathbf{b}}_2;\bar{\mathbf{x}}|p_2)\bar{G}(\mathbf{x};\mathbf{b}_2|p_2)$$
$$\times \bar{G}(\mathbf{b}_1;\mathbf{x'}|p_1)\,\bar{G}(\bar{\mathbf{x}}';\bar{\mathbf{b}}_1|p_1)\Big\rangle , \tag{3.9}$$

where $\Delta\mathbf{b}=\mathbf{b}_1-\mathbf{b}_2$ and $\Delta\bar{\mathbf{b}}=\bar{\mathbf{b}}_1-\bar{\mathbf{b}}_2$. The explicit form of the squared incoming wavefunction Φ is derived in appendix B.

In equation (3.9), we assume that the nuclear target has nonvanishing density only for some longitudinal positions $z_L>0$. The integration variables $\mathbf{b}_i$, $\bar{\mathbf{b}}_i$ denote the transverse boundary values of the Green's functions at the front end $z_L=0$ of the nuclear target. Fig. 3 gives a graphical representation for (3.9) which we shall heavily use in what follows. According to Fig. 3, the virtual photon wavefunction starts interacting with the nuclear medium at $z_L=0$ in both the amplitude and complex conjugate amplitude *after* dissociating at longitudinal positions $y_L,\bar{y}_L$ with $y_L,\bar{y}_L<0$. We emphasize, however, that despite appearance, equation (3.9) as well as its graphical representation in Fig. 3 also include the

case that the photon vertex dissociates inside the target at $y_L>0$. Technical details of how this is handled are given in appendix B.
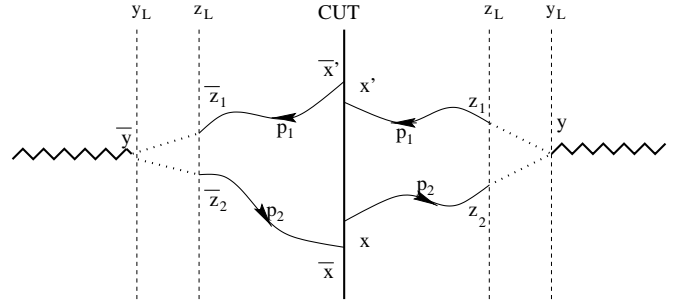

FIG. 3. Representation of the $\gamma^*\to q\bar{q}$ photodissociation cross section (3.6), (3.7). In the amplitude M_{fi}, the photon dissociates at position $(\mathbf{y},y_L)$ into a quark and an antiquark. These propagate with free non-interacting Green's functions (dotted lines) up to the front end of the target at longitudinal position z_L. From z_L onwards, the quark and antiquark are propagated inside the colour field with interacting Green's functions (full lines) up to their asympotic on-shell states ("cut"). For the complex conjugate amplitude, the analogous evolution of the hadronic $q\bar{q}$ Fock state is depicted on the other side of the cut.

IV. OPACITY EXPANSION AND COLOUR TRIVIALITY

In this section, we analyze the photoabsorption cross section (3.9) by expanding the interacting Green's functions $\bar{G}$ in powers of the scattering potential $A_0(\mathbf{x})$. In a first step, we focus on the total photoabsorption cross section

$$\sigma_{total}^{\gamma^*\to q\bar{q}} = \alpha_{\text{em}}\int d\alpha\int d\mathbf{b}_1\, d\mathbf{b}_2\, d\bar{\mathbf{b}}_1\, d\bar{\mathbf{b}}_2\, \Phi(\Delta\mathbf{b};\Delta\bar{\mathbf{b}};\alpha)$$
$$\times \Big\langle \int d\mathbf{x}_\perp\, \bar{G}(\bar{\mathbf{b}}_2;\mathbf{x}|p_2)\,\bar{G}(\mathbf{x};\mathbf{b}_2|p_2)$$
$$\times \int d\mathbf{x'}_\perp\, \bar{G}(\mathbf{b}_1;\mathbf{x'}|p_1)\,\bar{G}(\mathbf{x'};\bar{\mathbf{b}}_1|p_1)\Big\rangle . \tag{4.1}$$

To make sense of an expansion in powers of A_0, we have to specify the in medium average $\langle\ldots\rangle$ in terms of A_0. To this end, we specify for the colour potential (2.9) the contribution of a single scattering potential, centered at $(\check{\mathbf{r}}_i,\check{z}_i)$,

$$\varphi_i^a(\mathbf{x}_\perp,\xi) = \delta^{a\,a_i}\int \frac{d^3\boldsymbol{\kappa}}{(2\pi)^3}$$
$$\times a_0(\boldsymbol{\kappa}_\perp)\, e^{-i(\mathbf{x}_\perp-\check{\mathbf{r}}_i)\cdot\,\perp}e^{-i(\xi-\check{z}_i)\kappa^L} . \tag{4.2}$$

Here, we have approximated the argument of the single scattering potential $a_0(\boldsymbol{\kappa})\approx a_0(\boldsymbol{\kappa}_\perp)$. This implies that the momentum transfer occurs at a fixed longitudinal

position $\xi = \check{z}_i$. It is the standard approximation in the high energy limit where the dominant momentum transfer from the medium is transverse, and it motivates the use of time-ordered perturbation theory to rescattering problems [12,15].

Starting from (4.2), we define the medium average $\langle \ldots \rangle$ as an average over the transverse and longitudinal positions $(\check{\mathbf{r}}_i, \check{z}_i)$ of the scattering potentials and the colour factors a_i,

$$\langle f \rangle \equiv \frac{1}{A_\perp} \left(\prod_{i=1}^{N} \sum_{a_i} \int d\check{\mathbf{r}}_i \, d\check{z}_i \right) \\ \times f(\check{\mathbf{r}}_1, \ldots, \check{\mathbf{r}}_N; \check{z}_1, \ldots, \check{z}_N; a_1, \ldots, a_N). \quad (4.3)$$

Here, $A_\perp$ is a total transverse area which we divide out to regain the cross section per unit transverse area. N is the number of different single scattering potentials up to which the function f is expanded.

To simplify notation, we replace in what follows the discrete sum over $\check{z}_i$ in (2.10) by an integral over the density n of scattering centers

$$A_0(\mathbf{x}_\perp, \xi) = \int d\check{z}_i \, n(\check{z}_i) \, \varphi_i^a(\mathbf{x}_\perp, \xi) \, T^a. \quad (4.4)$$

Since the effective momentum transfer from the single potential $\varphi_i^a(\mathbf{x}_\perp, \xi)$ occurs at $\xi = \check{z}_i$, we shall often work with ξ as integration variable. The expansion of the photoabsorption cross section to N-th order in A_0 is an expansion in the N-th order of the opacity parameter $\alpha_s^2 \int d\xi \, n(\xi)$. In what follows, we study the perturbative expansion in this parameter.

A. N=1 result of Nikolaev and Zakharov

As a first illustration of the above formalism, we expand the integrand of the total photoabsorption cross section (4.1) to first order in the opacity parameter $\alpha_s^2 \int d\xi \, n(\xi)$, thereby reproducing the well-known nuclear shadowing result of Nikolaev and Zakharov. For $N = 1$, we have to expand all Green's functions in (4.1) and then to collect all contributions to order $O(A_0^2)$.

The zeroth and first order contributions $O(A_0^0)$ and $O(A_0^1)$ to $\sigma_{total}^{\gamma^* \to q\bar{q}}$ vanishes due to energy-momentum conservation: without momentum transfer to the medium, the q-$\bar{q}$-pair cannot appear on-shell. To second order $O(A_0^2)$, there are four different terms which we depict diagrammatically in Fig. 4a: for each term, the full lines correspond to the full lines shown in Fig. 3 and describe the full Green's functions in the total photoabsorption cross section (4.1). To simplify the representation, we have dropped in comparison to Fig. 3 the photon lines and incoming q-$\bar{q}$ wavefunctions. For the total photoabsorption cross section, the transverse positions at the cut

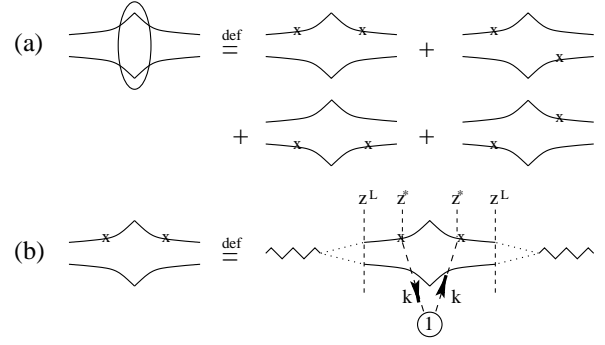are equal for the amplitude and the complex conjugate amplitude.

FIG. 4. (a) Diagrammatic representation of the $N = 1$ contribution to the total photoabsorption cross section (4.1). For each term, the upper (lower) line denotes the Green's function with energy p_1 (p_2) and the cusps denote the position of the cut. (b) Definition of the diagrammatic shorthand used in (a) and calculated in (4.5). Crosses stand for one power of the scattering potential A_0. The medium average ensures that the momentum flow k through the cut is conserved and that the potential A_0 is linked to the q-$\bar{q}$-system in M_{fi} and $M_{\text{fi}}^\dagger$ at the same longitudinal position.

Let us consider the first term on the r.h.s. of Fig. 4. Here, the Green's functions of argument p_2 are free while both Green's functions with argument p_1 are expanded to first order. Averaging over the position $(\check{\mathbf{r}}_1, \check{z}_1)$ of the center of the scattering potential, we find

$$\left\langle \int d\check{\mathbf{r}}_1 \, d\check{z}_1 \, d\mathbf{x}_\perp \, \bar{G}_0(\bar{\mathbf{b}}_2; \mathbf{x}|p_2) \, \bar{G}_0(\mathbf{x}; \mathbf{b}_2|p_2) \right. \\ \left. \times \int d\mathbf{x}'_\perp \, \bar{G}^{(1)}(\mathbf{b}_1; \mathbf{x}'|p_1) \, \bar{G}^{(1)}(\mathbf{x}'; \bar{\mathbf{b}}_1|p_1) \right\rangle \\ = \frac{1}{A_\perp} \int d\xi_1 \, n(\xi_1) \int \frac{d\boldsymbol{\kappa}_\perp}{(2\pi)^2} \, |a_0(\boldsymbol{\kappa}_\perp)|^2 \, T_{a_1} T_{a_1} \\ \times \delta^{(2)}(\bar{\mathbf{b}}_2 - \mathbf{b}_2) \, \delta^{(2)}(\bar{\mathbf{b}}_1 - \mathbf{b}_1). \quad (4.5)$$

This term does not depend on the separation between the q-$\bar{q}$ pair since the potential touches only one of the quark lines. In contrast, the second term on the r.h.s. of Fig. 4a depends on this separation and takes the explicit form

$$-\int d\xi_1 \, n(\xi_1) \int \frac{d\boldsymbol{\kappa}_\perp}{(2\pi)^2} \, |a_0(\boldsymbol{\kappa}_\perp)|^2 \, T_{a_1} T_{a_1} \, e^{-i\boldsymbol{\kappa}_\perp \cdot (\mathbf{r}_1 - \mathbf{r}_2)} \\ \times e^{-i\frac{\boldsymbol{\kappa}_\perp^2}{2\nu\alpha(1-\alpha)}(\xi_1 - z_L)} \, \delta^{(2)}\left(\bar{\mathbf{b}}_2 - \mathbf{b}_2 - \frac{\boldsymbol{\kappa}_\perp}{p_2}(\xi_1 - z_L)\right) \\ \times \delta^{(2)}\left(\bar{\mathbf{b}}_1 - \mathbf{b}_1 - \frac{\boldsymbol{\kappa}_\perp}{p_1}(\xi_1 - z_L)\right) \frac{1}{A_\perp}. \quad (4.6)$$

This shows explicitly that the transverse Brownian motion induced by rescattering is taken into account in our formulation: the q-$\bar{q}$ dipole does not propagate at fixed

transverse separation $\bar{\mathbf{b}}_1 - \mathbf{b}_1$ but changes its size in response to an interaction at the longitudinal position ξ_1 by terms of the form $\frac{\perp}{p_1}(\xi_1 - z_L)$. For $N = 1$, the first and only interaction takes place by definition at the position $z_L = \xi_1$ and these terms vanish. For $N > 1$, however, they do not vanish and lead to a nontrivial dynamical evolution of the transverse dipole size, see below.

Adding up the four real contributions in Fig. 4a, and doing the colour trace, we find

$$\sigma_{total}^{\gamma^* \to q\bar{q}}(N = 1) = N_c\,\alpha_{\rm em} \int d\xi\, n(\xi) \int d\alpha$$
$$\times \int d\mathbf{b}\, \Phi(\mathbf{b}; \mathbf{b}; \alpha)\, \sigma(\mathbf{b})\,, \qquad (4.7)$$

$$\sigma(\mathbf{b}) = 2\,C_F \int \frac{d\boldsymbol{\kappa}_\perp}{(2\pi)^2}\,|a_0(\boldsymbol{\kappa}_\perp)|^2\,\left(1 - e^{-i\,\perp\cdot\mathbf{b}}\right)\,. \qquad (4.8)$$

This is the result of Nikolaev and Zakharov [5]. The total cross section (4.1) is the product of the Born probability $\Phi(\mathbf{b}; \mathbf{b}; \alpha)$ for the incoming hadronic Fock state times a dipole cross section $\sigma(\mathbf{b})$, integrated over the transverse size $\mathbf{b}$ of the dipole and the energy distribution α between the quark and antiquark.

B. $N = 2$ tagged: non-trivial colour interference effects

As a second application of the opacity expansion, we consider the case of two tagged scattering centers. By this, we mean that (i) two scattering centers are involved in the process (4.1) and that (ii) two real momentum transfers occur in the medium. The 16 contributions to this $\sigma_{\rm tagged}^{\gamma^* \to q\bar{q}}(N = 2)$ are listed in Fig. 5. Summing them up, we find

$$\sigma_{\rm tagged}^{\gamma^* \to q\bar{q}}(N = 2)$$
$$= \alpha_{\rm em} \int d\xi_1\, n(\xi_1) \int_{\xi_1} d\xi_2\, n(\xi_2) \int d\alpha \int d\mathbf{b}$$
$$\times \int \frac{d\boldsymbol{\kappa}_{1,\perp}}{(2\pi)^2}\,\frac{d\boldsymbol{\kappa}_{2,\perp}}{(2\pi)^2}\,|a_0(\boldsymbol{\kappa}_{1,\perp})|^2\,|a_0(\boldsymbol{\kappa}_{2,\perp})|^2$$
$$\times \left(\mathrm{Tr}[a\,a\,b\,b]\,A^{(1)} + \mathrm{Tr}[a\,b\,a\,b]\,A^{(2)}\right)\,, \qquad (4.9)$$

where we have introduced the notational shorthands

$$A^{(1)} = 4\,\Phi(\mathbf{b}, \mathbf{b}; \alpha)\left(1 - e^{-i\,{}_{1,\perp}\cdot\mathbf{b}}\right)\,, \qquad (4.10)$$

$$A^{(2)} = 4\,\Phi\left(\mathbf{b} - \frac{\boldsymbol{\kappa}_{2,\perp}(\xi_2 - \xi_1)}{2\,\nu\,\alpha\,(1-\alpha)}, \mathbf{b} + \frac{\boldsymbol{\kappa}_{2,\perp}(\xi_2 - \xi_1)}{2\,\nu\,\alpha\,(1-\alpha)}; \alpha\right)$$
$$\times \left(e^{-i\,{}_{1,\perp}\cdot\mathbf{b}}e^{-i\frac{\boldsymbol{\kappa}_{1,\perp}\cdot\boldsymbol{\kappa}_{2,\perp}}{2\nu\alpha(1-\alpha)}(1-2\alpha)(\xi_2-\xi_1)}\right.$$
$$\left. -e^{-i\,{}_{1,\perp}\cdot\,{}_{2,\perp}\frac{(\xi_2-\xi_1)}{\nu\alpha}}\right)e^{-i\,{}_{2,\perp}\cdot\mathbf{b}}\,. \qquad (4.11)$$

Here, the term $A^{(2)}$ contains information about the non-trivial dynamical evolution of the q-$\bar{q}$-separation which

is determined by the "relative transverse mass" $\mu = \left(\frac{1}{p_1} - \frac{1}{p_2}\right)^{-1} = \nu\alpha(1-\alpha)$. The momentum transfer $\boldsymbol{\kappa}_{2,\perp}$ determines this change of the q-$\bar{q}$-size via a classical equation of motion: $\propto \frac{{}_{2,\perp}}{\mu}(\xi_2 - \xi_1)$. In the high energy limit $\nu \to \infty$, this transverse motion can be neglected and the q-$\bar{q}$-pair propagates at fixed separation. We find

$$\lim_{\nu \to \infty}\quad \sigma_{\rm tagged}^{\gamma^* \to q\bar{q}}(N = 2)$$

$$= \alpha_{\rm em} \int d\xi_1\, n(\xi_1) \int_{\xi_1} d\xi_2\, n(\xi_2) \int d\alpha \int d\mathbf{b}$$
$$\times \int \frac{d\boldsymbol{\kappa}_{1,\perp}}{(2\pi)^2}\,\frac{d\boldsymbol{\kappa}_{2,\perp}}{(2\pi)^2}\,|a_0(\boldsymbol{\kappa}_{1,\perp})|^2\,|a_0(\boldsymbol{\kappa}_{2,\perp})|^2$$
$$\times \Phi(\mathbf{b}, \mathbf{b}; \alpha)\,4\left(1 - e^{-i\,{}_{1,\perp}\cdot\mathbf{b}}\right)$$
$$\times \left(\mathrm{Tr}[a\,a\,b\,b] - \mathrm{Tr}[a\,b\,a\,b]\,e^{-i\,{}_{2,\perp}\cdot\mathbf{b}}\right)\,. \qquad (4.12)$$

Even in this limiting case, the colour algebra does not factorize from the momentum dependence. This is a consequence of the non-trivial colour interference between different photodissociation amplitudes. The photoabsorption cross section cannot be written as a function of the dipole cross section $\sigma(b)$. We note that this complication stems entirely from the non-abelianess of the problem. If we replace both colour traces in (4.12) by the same constant, the two $\boldsymbol{\kappa}_{i,\perp}$-integrations combine to the square of the dipole cross section (4.8). To sum up: in the tagged case, non-trivial colour interference effects prevent us from representing the photoabsorption cross section as a function of the dipole cross section.
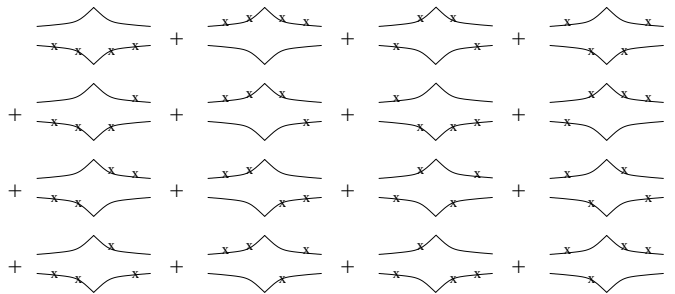

FIG. 5. The 16 contributions to the $N = 2$ photoabsorption cross section (4.9). In this "tagged" case, exactly two real momentum transfers occur on the amplitude level. The tagging gives rise to non-trivial colour interference effects.

C. Contact terms

In the calculation of the $N = 1$ cross section (4.7), we did not include all terms of the Taylor expansion of (4.1) to order $O(A_0^2)$. A second order contribution which was not included is e.g.

$$\left\langle \int d\check{\mathbf{r}}_1\,d\check{z}_1\,d\mathbf{x}_\perp\,\bar{G}_0(\bar{\mathbf{b}}_2; \mathbf{x}|p_2)\,\bar{G}_0(\mathbf{x}; \mathbf{b}_2|p_2)\right.$$

$$\times \int d\mathbf{x'}^\perp \bar{G}_0(\mathbf{b}_1;\mathbf{x'}|p_1)\,\bar{G}^{(2)}(\mathbf{x'};\bar{\mathbf{b}}_1|p_1)\Big\rangle$$

$$= -\frac{1}{2}\int d\xi_1\, n(\xi_1)\int \frac{d\boldsymbol{\kappa}_\perp}{(2\pi)^2}\,|a_0(\boldsymbol{\kappa}_\perp)|^2\,T_{a_1}\,T_{a_1}$$

$$\times \delta^{(2)}(\bar{\mathbf{b}}_2 - \mathbf{b}_2)\,\delta^{(2)}(\bar{\mathbf{b}}_1 - \mathbf{b}_1)\,. \qquad (4.13)$$

Here, the potential A_0 is linked two times to the complex conjugate amplitude and zero times to the amplitude. The medium average $\langle\ldots\rangle$ results in two important constraints: (i) both powers of A_0 couple to the q-$\bar{q}$-pair at the same longitudinal position ξ_1, and (ii) no net momentum is transferred to the q-$\bar{q}$- system. Scattering contributions with these properties were called *virtual* by Mueller and collaborators [4,26]. We refer to them as *contact terms*, all other interactions are refered to as *real*. Diagrammatically, the six contact terms for the $N = 1$ case are given in Fig. 6a, and equation (4.13) is represented by the first diagram on the r.h.s.
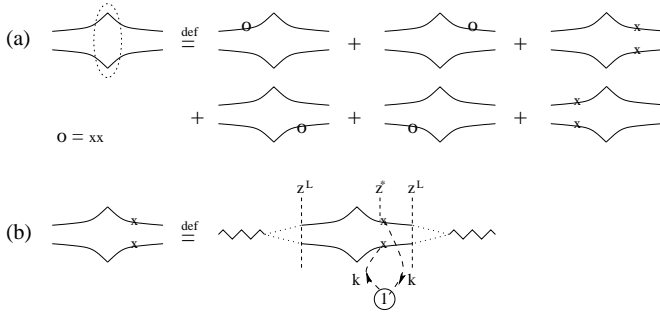

FIG. 6. (a) The six contact terms for the $N = 1$ scattering cross section. (b) Definition of the diagrammatic shorthand used in (a). The medium average ensures that (i) the momentum flow k is conserved and no net momentum is transferred to the q-$\bar{q}$-system, and that (ii) both powers of the scattering potential act at the same longitudinal position z^*.

For the $N = 1$ photoabsorption cross section (4.7), contact terms do not contribute since at least one interaction with the q-$\bar{q}$-system is needed in both the amplitude and complex conjugate amplitude in order to get the final state on shell. For $N > 2$, the same argument about energy-momentum conservation does not imply the absence of contact terms. We have to distinguish the following cases:

1. $\sigma_{\text{inel.}}^{\gamma^*\to q\bar{q}}$ inelastic: the cross section involves at least one real interaction.

2. $\sigma_{\text{diff.}}^{\gamma^*\to q\bar{q}}$ diffractive (or elastic): the medium interacts with the q-$\bar{q}$-pair only via contact terms.

3. $\sigma_{\text{total}}^{\gamma^*\to q\bar{q}}$ total: the cross section involves at least one (real or contact) interaction in both M_{fi} and $M_{fi}^\dagger$.

The notion "inelastic" is justified since any real interaction changes the colour of the target and thus affects

the hadronic activity between projectile and target rapidity (in this sense, the target "breaks up"). The notion "diffractive" or "elastic" involves an additional assumption: by construction, contact terms transfer exactly zero net transverse momentum to the q-$\bar{q}$-pair. Also, we regard in all calculations and for arbitrary scatterings the longitudinal momentum transfer as sufficiently small to justify the approximation $a_0(\boldsymbol{\kappa}) \approx a_0(\boldsymbol{\kappa}_\perp)$. Our assumption in the above definitions of the diffractive and total photoabsorption cross sections is that despite neglecting the longitudinal momentum transfer in all explicit calculations, it is sufficient to put the (extremely weakly off-shell) partonic contributions of γ^* on-shell. This is usually assumed in the calculation of the total [4] and diffractive [8] cross sections.

For $N > 1$, contact terms obviously play an important role in the calculation of the inelastic, diffractive and total photoabsorption cross section. In the remainder of this subsection, we summarize some of their important properties and shorthands, which will be heavily used in the following subsections:
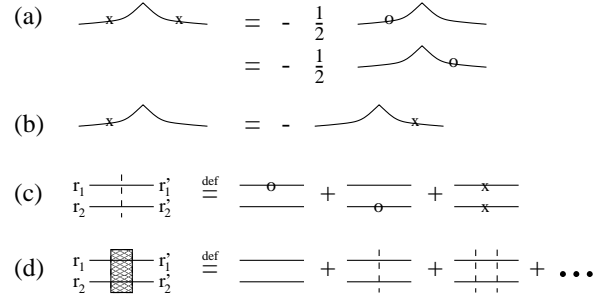

FIG. 7. At the cut, there are simple identities between real interaction terms and contact terms (a), and amongst real interaction terms (b). (c) A combination of the three possible contact terms at the same longitudinal position ξ leads to a dipole cross section $\sigma(\mathbf{r}_1(\xi) - \mathbf{r}_2(\xi))$ whose transverse size is evolved further with free Greens functions, see (4.14) (d) Iterating the combination of contact terms (c) leads to a dynamical evolution of the dipole size between initial transverse size $\mathbf{r}_1 - \mathbf{r}_2$ and final size $\mathbf{r}_1' - \mathbf{r}_2'$. This evolution is described by the path-integral (4.15).

1. Identities involving contact terms

First we observe that in (4.13), the Green's functions of momentum p_2 result in the transverse δ-function $\delta^{(2)}(\bar{\mathbf{b}}_2 - \mathbf{b}_2)$. Dropping them on both sides of (4.13), and observing that (4.13) and (4.5) differ by a factor $\frac{-1}{2}$, we have checked the identity in Fig. 7a. By a similar calculation, one also checks the identity Fig. 7b.

2. A path integral from iterating contact terms

We now consider the case in Fig. 7c, where the q-$\bar{q}$ state is evolved with exactly one contact term between longitudinal positions z and z' from a transverse separation $\mathbf{r}_1 - \mathbf{r}_2$ to a transverse separation $\mathbf{r}'_1 - \mathbf{r}'_2$. The sum over the three possible contact terms at longitudinal position ξ, represented on the r.h.s. of Fig. 7c, takes the explicit form

$$-\frac{T_a \cdots T_a}{2\,C_f} \int d\xi\, n(\xi) \int d\mathbf{r}_1(\xi)\, d\mathbf{r}_2(\xi)\, \sigma\left(\mathbf{r}_1(\xi) - \mathbf{r}_2(\xi)\right)$$

$$\times \bar{G}_0(\mathbf{r}_2, z; \mathbf{r}_2(\xi), \xi|p_2)\, \bar{G}_0(\mathbf{r}_2(\xi), \xi; \mathbf{r}'_2, z'|p_2)$$

$$\times \bar{G}_0(\mathbf{r}'_1, z'; \mathbf{r}_1(\xi), \xi|p_1)\, \bar{G}_0(\mathbf{r}_1(\xi), \xi; \mathbf{r}_2, z|p_1)\,. \quad (4.14)$$

Since Fig. 7c is only part of a more complicated Feynman diagram, we can say nothing about the positioning of the colour factors T_a. The corresponding expression $T_a \cdots T_a$ in (4.14) is purely formal. However, for the following, we anticipate an argument explained in the next subsection: for our purposes, the colour factors reduce to a Casimir factor C_F, i.e., we can substitute in (4.14) $\frac{T_a \cdots T_a}{C_f} \to 1$. Then, equation (4.14) is seen to correspond to the first order $n(\xi)$ density expansion of the double path integral (for $z' > z$)

$$M(\mathbf{r}_1, \mathbf{r}_2, z; \mathbf{r}'_1, \mathbf{r}'_2, z'|\alpha|\nu)$$

$$= \int\limits_{\mathbf{r}_1(z)=\mathbf{r}_1}^{\mathbf{r}_1(z')=\mathbf{r}'_1} \mathcal{D}\mathbf{r}_1 \int\limits_{\mathbf{r}_2(z)=\mathbf{r}_2}^{\mathbf{r}_2(z')=\mathbf{r}'_2} \mathcal{D}\mathbf{r}_2$$

$$\times \exp\left\{ i \int_z^{z'} d\bar{\xi}\, \frac{\nu}{2}\left(\alpha\,\dot{\mathbf{r}}_2^2 + (1-\alpha)\,\dot{\mathbf{r}}_1^2\right)\right.$$

$$\left. + i\frac{1}{2}\,n(\xi)\,\sigma\left(\mathbf{r}_1(\xi) - \mathbf{r}_2(\xi)\right)\right\}\,. \quad (4.15)$$

Moreover, the expansion of (4.15) to m-th order in the density $n(\xi)$ corresponds exactly to the m-th term on the r.h.s. of Fig. 7d. This shows that the iteration Fig. 7d of the one contact term interaction Fig. 7d is described by the path-integral (4.15). Since this path integral plays an important role in what follows, we simplify it further. Using the coordinate transformation

$$\mathbf{r}_a(\xi) = (1-\alpha)\,\mathbf{r}_1(\xi) + \alpha\,\mathbf{r}_2(\xi)\,, \quad (4.16)$$

$$\mathbf{r}_b(\xi) = \mathbf{r}_1(\xi) - \mathbf{r}_2(\xi)\,, \quad (4.17)$$

we can write

$$M(\mathbf{r}_1, \mathbf{r}_2, z; \mathbf{r}'_1, \mathbf{r}'_2, z'|\alpha|\nu)$$
$$= \mathcal{K}_0\left(\mathbf{r}_a(z'), z'; \mathbf{r}_a(z), z|\nu\right)$$
$$\times \mathcal{K}\left(\mathbf{r}_b(z'), z'; \mathbf{r}_b(z), z|\nu\alpha(1-\alpha)\right)\,. \quad (4.18)$$

The path-integral on the r.h.s. of this expression is given by (for $z' > z$)

$$\mathcal{K}\left(\mathbf{r}(z'), z'; \mathbf{r}(z), z|\mu\right)$$

$$= \int \mathcal{D}\mathbf{r}\, \exp\left\{ i \int_z^{z'} d\xi\, \left[\frac{\mu}{2}\dot{\mathbf{r}}^2 + i\frac{1}{2}n(\xi)\,\sigma\left(\mathbf{r}\right)\right]\right\}\,. \quad (4.19)$$

Its opacity expansion reads

$$\mathcal{K}(\mathbf{r}', z'; \mathbf{r}, z) = \mathcal{K}_0(\mathbf{r}', z'; \mathbf{r}, z) =$$

$$- \int_z^{z'} d\xi \int d\boldsymbol{\rho}\, \mathcal{K}_0(\mathbf{r}', z'; \mathbf{r}, \xi)\, \Sigma\left(\boldsymbol{\rho}, \xi\right) \mathcal{K}_0(\boldsymbol{\rho}, \xi; \mathbf{r}, z)$$

$$+ \int_z^{z'} d\xi_1 \int_{\xi_1}^{z'} d\xi_2 \int d\boldsymbol{\rho}_1\, d\boldsymbol{\rho}_2\, \mathcal{K}_0(\mathbf{r}', z'; \boldsymbol{\rho}_2, \xi_2)\, \Sigma\left(\boldsymbol{\rho}_2, \xi_2\right)$$

$$\times \mathcal{K}(\boldsymbol{\rho}_2, \xi_2; \boldsymbol{\rho}_1, \xi_1)\, \Sigma\left(\boldsymbol{\rho}_1, \xi_1\right) \mathcal{K}_0(\boldsymbol{\rho}_1, \xi_1; \mathbf{r}, z)\,, \quad (4.20)$$

where $\Sigma\left(\boldsymbol{\rho}, \xi\right) = \frac{1}{2}\,n(\xi)\sigma\left(\boldsymbol{\rho}\right)$. Here, we have suppressed the explicit μ-dependence in $\mathcal{K}$. The corresponding free Green's function $\mathcal{K}_0$ reads

$$\mathcal{K}_0(\mathbf{r}', z'; \mathbf{r}, z) = \frac{\mu}{2\pi\, i\, (z'-z)}\,\exp\left\{\frac{i\mu\,(\mathbf{r}'-\mathbf{r})^2}{2\,(z'-z)}\right\}\,. \quad (4.21)$$

In analogy to our definition of the Green's function $\bar{G}$ in (2.16), we define $\mathcal{K}\left(\mathbf{r}(z), z; \mathbf{r}(z'), z'|\mu\right) \equiv \mathcal{K}^\dagger\left(\mathbf{r}(z'), z'; \mathbf{r}(z), z|\mu\right)$ for $z' > z$.

A path integral $\mathcal{K}$ of the form derived here was first used by Zakharov in the abelian problem of calculating the passage of ultrarelativistic positronium through matter [31]. More recently, the same path integral was shown to appear in the final expression of the medium-dependence of the LPM-bremsstrahlung spectrum [14,21].

D. $N =$ arbitrary, untagged: contact terms remove colour interference effects

What happens if contact terms are included in the $N = 2$ calculation of the elastic, inelastic and total photoabsorption cross section? In Fig. 8, we have classified into four subsets all terms of order $O(n(\xi)^2)$ which have to be considered for the $N = 2$ photoabsorption cross sections. There are in Fig. 8a the $4 \times 4 = 16$ terms for which both interactions are real, in Fig. 8b the $4 \times 6 = 24$ terms for which only the second interaction is contact, in Fig. 8c the $3 \times 4 \times 2$ terms for which only the first interaction is contact, and in Fig. 8d the $2 \times 3 \times 6 = 36$ which involve two contact interactions. All together, these are 100 terms. For the total and the inelastic cross section, the terms in Fig. 8a and Fig. 8b both contribute, but they cancel each other exactly. More precisely, the first diagram in Fig. 8a cancels the first diagram in Fig. 8b, the

second diagram in Fig. 8a cancels the second diagram in Fig. 8b, etc. This is a consequence of the identities Fig. 7a and 7b which we apply to the last interaction before the cut.
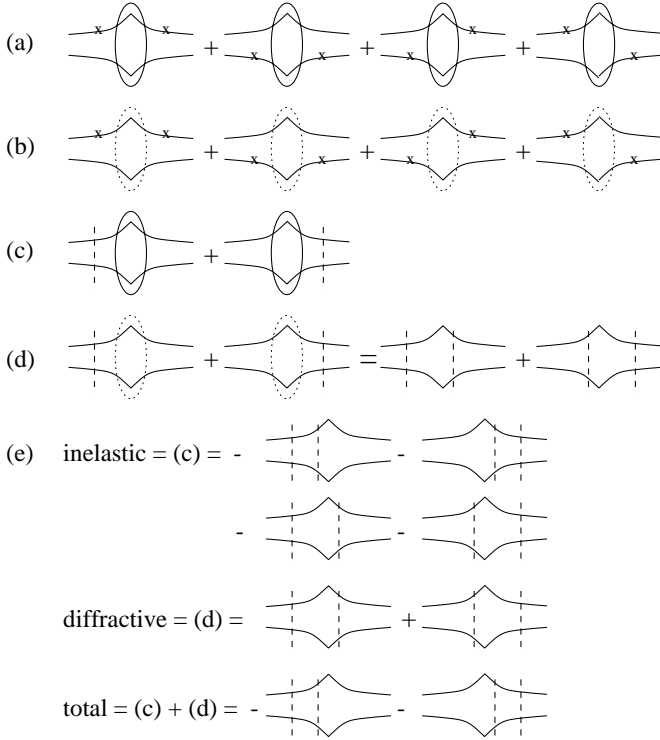

FIG. 8. The contributions to the $N = 2$ photoabsorption cross section: (a) the 16 real contributions which are present in the "tagged" case. (b) Contributions for which the first interaction is real and the second a contact term. (c) Contributions for which the first interaction is a contact term and the second interaction transfers momentum. (d) Terms which contain two contact interactions. Here, energy-momentum conservation ensures that the two contact terms do not stand on the same side of the cut. (e) Inelastic, diffractive and total photoabsorption cross section are determined by different combinations of the contributions (c) and (d). Rewriting the real interaction in (c) as the sum of two negative contact term contributions, a particularly simple representation is obtained.

The same argument cannot be made for the cancellation of the diagrams in Fig. 8c and Fig. 8d: energy momentum conservation restricts the occurence of double contact terms, since at least one interaction is needed on the amplitude level to get the final state on-shell. Depending on whether we calculate the diffractive, inelastic or total photoabsorption cross section, different combinations of these two sets of diagrams contribute. The real interaction Fig. 4a at the cut is determined by minus the combination Fig. 6a of contact terms. This allows us to express all three contributions to the photoabsorption cross section in terms of contact terms, as shown in

Fig. 8. Most importantly, all contributions to these photoabsorption cross sections have the colour trace $\mathrm{Tr}[aabb]$: for the untagged case for which contact terms are included, colour interference terms vanish in the diffractive, inelastic and total $N = 2$ photoabsorption cross section.

The above argument can be generalized easily to arbitrary N. As shown in Fig. 9a, whenever at least one of the $(N-1)$ first interactions is real, the sum of all real and virtual terms for the N-th interaction cancels. Inelastic, diffractive and total photoabsorption cross section can thus again be described in terms of $(N-1)$ contact terms and a characteristic N-th contribution at the cut. As an immediate consequence, the colour trace of all these contributions reads

$$\mathrm{Tr}[T_{a_1} T_{a_2} \ldots T_{a_N} T_{a_N} T_{a_{N-1}} \ldots T_{a_1}] = N_c\, C_F^N \ . \quad (4.22)$$

In contrast to the tagged photoabsorption cross section, the colour structure factorizes from the momentum dependence: Inclusion of the contact terms results in colour triviality for the N-fold diffractive, inelastic and total photoabsorption cross section. This justifies the assumption made in deriving the path integral (4.15) in the last subsection.
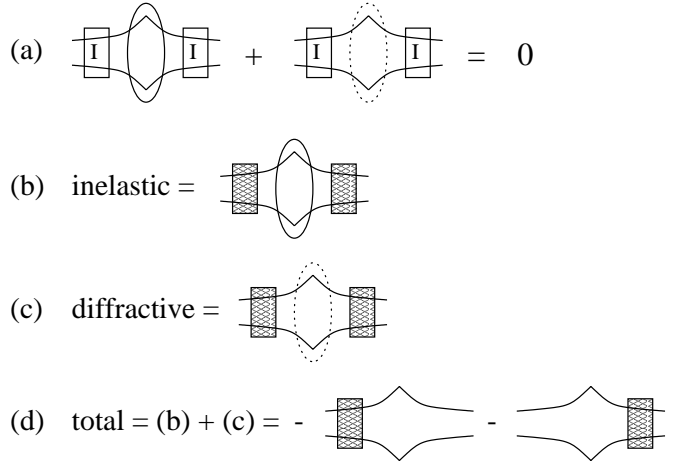

FIG. 9. (a) Cancellation of real and contact terms for any combination of interactions [I] which contains at least one real or contact interaction. (b)-(d) The identity (a) allows for the generalization to arbitrary N of the $N = 2$ photoabsorption cross section of Fig. 8.

According to Fig. 9(b)-(d), the inelastic, diffractive and total photabsorption cross section can be written in terms of the path-integral $\mathcal{K}$ of (4.19) which describes the iteration of contact terms. For the inelastic photoabsorption cross section, this leads to the expression

$$\sigma_{\mathrm{inel.}}^{\gamma^* \to q\bar{q}} = N_c\, \alpha_{\mathrm{em}} \int d\alpha \int d\mathbf{b}\, d\bar{\mathbf{b}}$$

$$\times \Phi\left(\mathbf{b}; \bar{\mathbf{b}}; \alpha\right) \int_{\xi_{nl}}^{L} d\xi\, n(\xi) \int d\mathbf{r}(\xi)$$

11

$$\times \mathcal{K}\big(\bar{\mathbf{b}}, 0; \mathbf{r}(\xi), \xi | \nu\alpha(1-\alpha)\big)\, \sigma\big(\mathbf{r}(\xi)\big)$$
$$\times \mathcal{K}\big(\mathbf{r}(\xi), \xi; \mathbf{b}, 0 | \nu\alpha(1-\alpha)\big) . \qquad (4.23)$$

Here, the Green's functions $\mathcal{K}$ describe the propagation of the q-$\bar{q}$-dipole from the front end of the target at $z = 0$ up to the position ξ of the last interaction. The lower boundary ξ_{nl} of the integration over ξ is defined by the position of the next to last ("nl") interaction. This is an awkward property, since we have to expand the $\mathcal{K}$'s in the number N of interactions to determine ξ_{nl} order for order in N. This makes it important to find for (4.23) with the help of the opacity expansion (4.20) the equivalent representation

$$\sigma^{\gamma^* \to q\bar{q}}_{\text{inel.}} = N_c\, \alpha_{\text{em}} \int d\alpha \int d\mathbf{b}\, d\bar{\mathbf{b}}\, \Phi\left(\mathbf{b}; \bar{\mathbf{b}}; \alpha\right)$$
$$\times \Big[\delta^{(2)}\left(\mathbf{b} - \bar{\mathbf{b}}\right)$$
$$- \int d\mathbf{r}_e\, \mathcal{K}\big(\bar{\mathbf{b}}, 0; \mathbf{r}_e, L | \mu\big)\, \mathcal{K}\big(\mathbf{r}_e, L; \mathbf{b}, 0 | \mu\big) \Big] . \quad (4.24)$$

For the diffractive contribution, one finds

$$\sigma^{\gamma^* \to q\bar{q}}_{\text{diff.}} = N_c\, \alpha_{\text{em}} \int d\alpha \int d\mathbf{b}\, d\bar{\mathbf{b}}\, \Phi\left(\mathbf{b}; \bar{\mathbf{b}}; \alpha\right) \int d\mathbf{r}_e$$
$$\times \Big[\delta^{(2)}\left(\bar{\mathbf{b}} - \mathbf{r}_e\right) - \mathcal{K}\big(\bar{\mathbf{b}}, 0; \mathbf{r}_e, L | \mu\big) \Big]$$
$$\times \Big[\delta^{(2)}\left(\mathbf{r}_e - \mathbf{b}\right) - \mathcal{K}\big(\mathbf{r}_e, L; \mathbf{b}, 0 | \mu\big) \Big] . \qquad (4.25)$$

The total photoabsorption cross section is the sum of both

$$\sigma^{\gamma^* \to q\bar{q}}_{\text{total}} = N_c\, \alpha_{\text{em}} \int d\alpha \int d\mathbf{b}\, d\bar{\mathbf{b}}\, \Phi\left(\mathbf{b}; \bar{\mathbf{b}}; \alpha\right)$$
$$\times \Big[2\, \delta^{(2)}\left(\bar{\mathbf{b}} - \mathbf{b}\right) - \mathcal{K}\big(\bar{\mathbf{b}}, 0; \mathbf{b}, L | \mu\big)$$
$$- \mathcal{K}\big(\bar{\mathbf{b}}, L; \mathbf{b}, 0 | \mu\big) \Big] . \qquad (4.26)$$

Before turning in the next subsection to the discussion of these expressions, we remark shortly on a phase convention implicitly used in the above results:

The first $(N-1)$ interactions in the above photoabsorption cross sections are contact terms. Contact terms stand either to the right or to the left of the cut. The first interaction thus occurs for each non-vanishing contribution to (4.24) at *different* longitudinal positions z_a, z_b in the amplitude and complex conjugate amplitude. As a consequence, the free incoming wavefunction has to be evolved to these different positions in M_{fi} and $M_{\text{fi}}^\dagger$. We explain in Appendix B following (B8) that the expression Φ for the squared incoming wavefunction is only correct as long as $z_a = z_b$. If one insists on using Φ for $z_a \neq z_b$, one is forced to adopt the phase convention:

$$\int d\bar{\mathbf{b}}\, \Phi\left(\mathbf{b}; \bar{\mathbf{b}}; \alpha\right)\, \mathcal{K}_0\big(\bar{\mathbf{b}}, z_a; \bar{\mathbf{r}}, z_b | \nu\alpha(1-\alpha)\big)$$
$$= \Phi\left(\mathbf{b}; \bar{\mathbf{r}}; \alpha\right)\, e^{-i\, q\, (z_b - z_a)} . \qquad (4.27)$$

Strictly speaking, using Φ one has done the y_L- and $\bar{y}_L$-integrations in the photodissociation probability (3.7) *before* specifying the true endpoints of these integrations which are given by the positions z_a, z_b of the first interactions in M_{fi} and $M_{\text{fi}}^\dagger$. The phase convention (4.27) corrects for the part of the y_L integral which one misses in assuming $z_a = z_b$. Here, we shortly illustrate the consequences of (4.27):

With the help of (4.27), one checks immediately that the $N = 1$ contribution to (4.24) agrees with the result (4.7) of Nikolaev and Zakharov. There is no additional phase factor in this case since $z_a = z_b$. However, there is an additional phase factor for all contributions $N > 1$. In the notationally simplest case, $N = 2$, we find

$$\sigma^{\gamma^* \to q\bar{q}}_{inel.}(N = 2)$$
$$= -N_c\, \alpha_{\text{em}}\, \text{Re} \int d\alpha \int d\xi'\, n(\xi') \int_{\xi'} d\xi n(\xi)$$
$$\times \int d\mathbf{r}\, d\bar{\mathbf{r}}\, \Phi\left(\mathbf{r}; \bar{\mathbf{r}}; \alpha\right)\, e^{iq(\xi - \xi')}$$
$$\times \sigma\left(\bar{\mathbf{r}}\right) \mathcal{K}_0\big(\bar{\mathbf{r}}, \xi'; \mathbf{r}, \xi | \mu\big)\, \sigma\left(\mathbf{r}\right) . \qquad (4.28)$$

The phase factor $\exp\{iq\,(\xi - \xi')\}$ is sensitive to the difference between the longitudinal position of the first scattering center in M_{fi} and $M_{\text{fi}}^\dagger$. The scale is set by the inverse coherence length

$$q = \frac{Q^2}{2\nu} - \frac{m^2}{2\nu\alpha(1-\alpha)} = \frac{1}{l_f} . \qquad (4.29)$$

It can be neglected in the high energy limit $\nu \to \infty$ where the longitudinal extension of the target becomes small compared to $1/q$.

E. Colour triviality of the one-fold differential photoabsorption cross section

Colour triviality of the inelastic, diffractive and total photoabsorption cross section (4.24)-(4.26) is the result of a complete diagrammatic cancellation which arises due to the identities in Fig. 7 (a) and (b). These identities are stronger than implied by the optical theorem since they are based only on the transverse momentum integration of one of the two quarks in the final state. This makes it possible to use them in the simplification of more differential observables. Here, we study the one-fold differential photoabsorption cross section

$$\frac{d\sigma^{\gamma^* \to q\bar{q}}}{d\alpha\, d\mathbf{p}_1^\perp} = \frac{\alpha_{\text{em}}}{(2\pi)^2} \int d\mathbf{b}_1\, d\mathbf{b}_2\, d\bar{\mathbf{b}}_1\, d\bar{\mathbf{b}}_2\, \Phi(\Delta\mathbf{b}; \Delta\bar{\mathbf{b}}; \alpha)$$
$$\times \int d\mathbf{x}_\perp\, d\mathbf{x}'_\perp\, d\bar{\mathbf{x}}'_\perp\, e^{i\, \mathbf{p}_1^\perp \cdot (\mathbf{x}'_\perp - \bar{\mathbf{x}}'_\perp)}$$
$$\times \Big\langle \bar{G}(\bar{\mathbf{b}}_2; \mathbf{x} | p_2) \bar{G}(\mathbf{x}; \mathbf{b}_2 | p_2)$$
$$\times \bar{G}(\mathbf{b}_1; \mathbf{x}' | p_1)\, \bar{G}(\bar{\mathbf{x}}'; \bar{\mathbf{b}}_1 | p_1) \Big\rangle . \qquad (4.30)$$

We shall derive for the inelastic part of (4.30) an expression in terms of

$$\bar{\sigma}(\mathbf{b}) = 2\,C_F \int \frac{d\boldsymbol{\kappa}_\perp}{(2\pi)^2}\,|a_0(\boldsymbol{\kappa}_\perp)|^2\,e^{-i\,\boldsymbol{\kappa}_\perp\cdot\mathbf{b}}\,, \qquad (4.31)$$

which is closely related to the dipole cross section,

$$\sigma(\mathbf{r}_1 - \bar{\mathbf{r}}_1) = \bar{\sigma}(0) - \bar{\sigma}\left(\mathbf{r}_1 - \bar{\mathbf{r}}_1\right)\,. \qquad (4.32)$$

The term $\bar{\sigma}(0)$ corresponds to a contact term for which both vertices are linked to the same quark of the q-$\bar{q}$-system. In intermediate steps of our calculation, $\bar{\sigma}$ is a useful bookkeeping device to evaluate the diagrams in Fig. 10a. Our final result, however, will depend only on the dipole cross section.

1. Inelastic one-fold differential cross section

The diagrammatic book-keeping of the inelastic contributions to the one-fold differential cross section (4.30) are involved. In appendix C, we classify all contributing diagrams and we use the identities Fig. 7a and b to show that many of these diagrams cancel each other. As a result of this analysis, the remaining non-vanishing contributions can be represented by the diagrams in Fig. 10a. The colour trace for the N-th order terms of all these diagrams is $N_c\,C_F^N$: the inelastic part of the cross section (4.30) is thus free of colour interference terms, it is colour trivial.
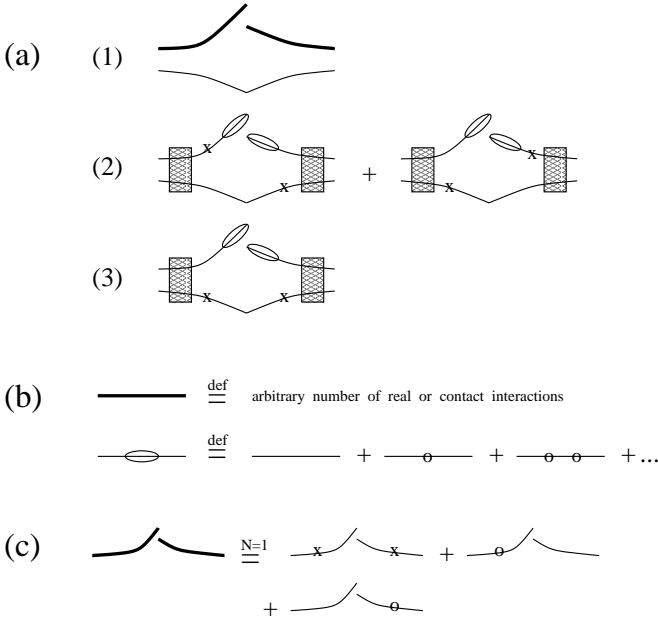

(a) (1)

(2)

(3)

(b)

(c)

FIG. 10. (a) The non-vanishing contributions to the inelastic part of the one-fold differential photoabsorption cross section (4.30) as classified in appendix C. (b) Definition of diagrammatic shorthands used in (a). (c) Order $N = 1$ contribution to (a1).

We start with the $N = 1$ contribution to the diagram Fig. 10a1.

$$e^{i\mathbf{p}_1^\perp\cdot(\mathbf{x}'-\bar{\mathbf{x}}')} \int_0^L d\xi\,\frac{n(\xi)}{2}\,\left[\bar{\sigma}\left(\mathbf{r}_1 - \bar{\mathbf{r}}_1\right) - \bar{\sigma}(0)\right]\Big|_{\mathbf{r}_1-\bar{\mathbf{r}}_1=\mathbf{x}'-\bar{\mathbf{x}}'}\,. \qquad (4.33)$$

This contribution is shown explicitly in Fig. 10c. The relative transverse separation $\mathbf{r}_1 - \bar{\mathbf{r}}_1$ between the quark in the amplitude and complex conjugated amplitude does not change with longitudinal position ξ. This is a consequence of evolving on both sides of the cut with Green's functions of same energy p_1. It makes the iteration of the $N = 1$ contribution to arbitrary high orders particularly easy. The total contribution to Fig. 10a1 reads

$$e^{i\mathbf{p}_1^\perp\cdot\left(\mathbf{x}'-\bar{\mathbf{x}}'\right)}\left(e^{-\int_0^L d\xi\,\frac{n(\xi)}{2}\,\sigma\left(\mathbf{x}'-\bar{\mathbf{x}}'\right)} - e^{-\int_0^L d\xi\,\frac{n(\xi)}{2}\,\bar{\sigma}(0)}\right)\,. \qquad (4.34)$$

The first term is just the exponentiation of the $N = 1$- contribution. The second term subtracts those N-th order contributions which involve only contact terms and thus do not add to the inelastic contribution.

To evaluate the three contributions in Fig. 10a2 and a3, we assume that the real momentum transfer occurs at an arbitrary but fixed longitudinal position $\check{\xi}$. The evolution of the free incoming Fock state up to $\check{\xi}$ is then described by the path-integral (4.18). The part of the expression for $\xi > \check{\xi}$ is given by

$$e^{i\mathbf{p}_1^\perp\cdot\left(\mathbf{r}_1(\check{\xi})-\bar{\mathbf{r}}_1(\check{\xi})\right)}\,e^{-\int_{\check{\xi}}^L d\xi\,\frac{n(\xi)}{2}\,\bar{\sigma}(0)}$$
$$\times\left[\sigma\left(\bar{\mathbf{r}}_2(\check{\xi}) - \bar{\mathbf{r}}_1(\check{\xi})\right) + \sigma\left(\mathbf{r}_2(\check{\xi}) - \mathbf{r}_1(\check{\xi})\right) - \bar{\sigma}(0)\right]\,. \quad (4.35)$$

Here, the real interactions at $\check{\xi}$ combine to the second line of (4.35) and the arbitrary number of contact terms at $\xi > \check{\xi}$ leads to the exponential of $\bar{\sigma}(0)$. Adding up all contributions of Fig. 10a, we find for the differential photoabsorption cross section (4.30):

$$\frac{d\sigma_{\text{inel.}}^{\gamma^*\to q\bar{q}}}{d\alpha\,d\mathbf{p}_1^\perp}$$
$$= \frac{\alpha_{\text{em}}\,N_c}{(2\pi)^2} \int d\mathbf{b}\,d\bar{\mathbf{b}}\,\Phi(\mathbf{b};\bar{\mathbf{b}};\alpha)$$
$$\times\left[e^{i\,\mathbf{p}_1^\perp\cdot(\mathbf{b}-\bar{\mathbf{b}})}\left(e^{-\int_0^L d\xi\,\frac{n(\xi)}{2}\,\sigma\left(\mathbf{b}-\bar{\mathbf{b}}\right)}\right.\right.$$
$$\left.-e^{-\int_0^L d\xi\,\frac{n(\xi)}{2}\,\bar{\sigma}(0)}\right)$$
$$+ \int_{\xi_{nl}}^L d\check{\xi}\,\frac{n(\check{\xi})}{2} \int d\mathbf{r}\,d\bar{\mathbf{r}}\,\mathcal{K}(\bar{\mathbf{b}},0;\bar{\mathbf{r}},\check{\xi}|\mu)$$
$$\times\{\sigma(\bar{\mathbf{r}}) + \sigma(\mathbf{r}) - \bar{\sigma}(0)\}\,\mathcal{K}(\mathbf{r},\check{\xi};\mathbf{b},0|\mu)$$
$$\times\,e^{-\int_{\check{\xi}}^L d\xi\,\frac{n(\xi)}{2}\,\bar{\sigma}(0)}\,e^{i\,\mathbf{p}_1^\perp\cdot(\mathbf{r}-\bar{\mathbf{r}})}\bigg]\,. \qquad (4.36)$$

13

The first term in the wide brackets stems from the contribution Fig. 10a1) given in (4.34), the second term denotes the diagrams Fig. 10a2) and a3). Here, the Green's functions $\mathcal{K}$ describe the dynamical evolution of the q-$\bar{q}$ dipoles up to the real interaction at $\check{\xi}$, from which point onwards the dynamics is given by (4.35). In analogy to (4.23), the lower boundary ξ_{nl} of the intergration over $\check{\xi}$ is determined by the last interaction point before the real interaction. To remove this indirectly defined variable from our solution, we use again the opacity expansion (4.20) to show that

$$
\frac{d\sigma_{\text{inel.}}^{\gamma^* \to q\bar{q}}}{d\alpha\, d\mathbf{p}_1^\perp} = \frac{\alpha_{\text{em}} N_c}{(2\pi)^2} \int d\mathbf{b}\, d\bar{\mathbf{b}}\, \Phi(\mathbf{b}; \bar{\mathbf{b}}; \alpha)
$$
$$
\times \left[e^{i\, \mathbf{p}_1^\perp \cdot (\mathbf{b} - \bar{\mathbf{b}})}\, e^{-\int_0^L d\xi\, \frac{n(\xi)}{2}\, \sigma(\mathbf{b} - \bar{\mathbf{b}})} - \int d\mathbf{r}\, d\bar{\mathbf{r}} \right.
$$
$$
\left. e^{i\, \mathbf{p}_1^\perp \cdot (\mathbf{r} - \bar{\mathbf{r}})}\, \mathcal{K}(\bar{\mathbf{b}}, 0; \bar{\mathbf{r}}, L | \mu)\, \mathcal{K}(\mathbf{r}, L; \mathbf{b}, 0 | \mu) \right] \,. \quad (4.37)
$$

It is easy to check that the $\mathbf{p}_1^\perp$-integration of this expression coincides with the incluse inelastic photoabsorption cross section (4.24).

2. Diffractive and total photoabsorption cross section with one jet resolved

The diffractive one-fold differential photoabsorption cross section involves by definition only contact terms. Due to energy momentum conservation, at least one contact term is required on the amplitude level. An arbitrary non-vanishing number of contact terms in the amplitude translates into a factor $\delta - \mathcal{K}$, see the discussion of Fig. 7 (d). Hence, the diffractive contribution to the cross section reads

$$
\frac{d\sigma_{\text{diff.}}^{\gamma^* \to q\bar{q}}}{d\alpha\, d\mathbf{p}_1^\perp} = \frac{\alpha_{\text{em}} N_c}{(2\pi)^2} \int d\mathbf{b}\, d\bar{\mathbf{b}}\, \Phi(\mathbf{b}; \bar{\mathbf{b}}; \alpha) \int d\mathbf{r}\, d\bar{\mathbf{r}}\, e^{i\, \mathbf{p}_1^\perp \cdot (\mathbf{r} - \bar{\mathbf{r}})}
$$
$$
\times \left[\delta^{(2)}(\bar{\mathbf{b}} - \bar{\mathbf{r}}) - \mathcal{K}(\bar{\mathbf{b}}, 0; \bar{\mathbf{r}}, L | \mu) \right]
$$
$$
\times \left[\delta^{(2)}(\mathbf{b} - \mathbf{r}) - \mathcal{K}(\mathbf{r}, L; \mathbf{b}, 0 | \mu) \right] \,. \quad (4.38)
$$

The one-fold differential total cross section is given by the sum of the contributions (4.37) and (4.38),

$$
\frac{d\sigma_{\text{total}}^{\gamma^* \to q\bar{q}}}{d\alpha\, d\mathbf{p}_1^\perp} = \frac{\alpha_{\text{em}} N_c}{(2\pi)^2} \int d\mathbf{b}\, d\bar{\mathbf{b}}\, \Phi(\mathbf{b}; \bar{\mathbf{b}}; \alpha)
$$
$$
\times \left[e^{i\, \mathbf{p}_1^\perp \cdot (\mathbf{b} - \bar{\mathbf{b}})} \left(e^{-\int_0^L d\xi\, \frac{n(\xi)}{2}\, \sigma(\mathbf{b} - \bar{\mathbf{b}})} + 1 \right) \right.
$$
$$
- \int d\mathbf{r}\, e^{i\, \mathbf{p}_1^\perp \cdot (\mathbf{r} - \bar{\mathbf{b}})}\, \mathcal{K}(\mathbf{r}, L; \mathbf{b}, 0 | \mu)
$$
$$
\left. - \int d\bar{\mathbf{r}}\, e^{i\, \mathbf{p}_1^\perp \cdot (\mathbf{b} - \bar{\mathbf{r}})}\, \mathcal{K}(\bar{\mathbf{b}}, 0; \bar{\mathbf{r}}, L | \mu) \right] \,. \quad (4.39)
$$

3. Non-trivial colour interference in one-fold and two-fold differential photoabsorption cross sections

Colour triviality of differential cross sections cannot be taken for granted. It has to be established by the diagrammatic techniques used in the above subsections. To illustrate this point, we give in the following simple examples of untagged differential cross sections which show colour interference effects. We calculate the inelastic part of the $N = 2$ photoabsorption cross section (3.9) in the $\nu \to \infty$ limit in which the q-$\bar{q}$ state propagates along straight lines through the nuclear target. For a target of thickness L and homogeneous density $n(\xi) = n_0$,

$$
\frac{d\sigma_{\text{inel.}}^{\gamma^* \to q\bar{q}}(N = 2)}{d\alpha\, d\mathbf{p}_1^\perp\, d\mathbf{p}_2^\perp}
$$
$$
= \frac{\alpha_{\text{em}}}{(2\pi)^4} \int d\mathbf{b}_1\, d\mathbf{b}_2\, d\bar{\mathbf{b}}_1\, d\bar{\mathbf{b}}_2\, \Phi(\mathbf{b}_1 - \mathbf{b}_2; \bar{\mathbf{b}}_1 - \bar{\mathbf{b}}_2; \alpha)
$$
$$
\times e^{i\, \mathbf{p}_1^\perp \cdot (\mathbf{b}_1 - \bar{\mathbf{b}}_1)}\, e^{-i\, \mathbf{p}_2^\perp \cdot (\mathbf{b}_2 - \bar{\mathbf{b}}_2)}\, \frac{n_0^2\, L^2}{2\, C_F^2}\, \frac{1}{4}
$$
$$
\times \left[\bar{\sigma}(\mathbf{b}_1 - \bar{\mathbf{b}}_1) + \bar{\sigma}(\mathbf{b}_2 - \bar{\mathbf{b}}_2) \right.
$$
$$
\left. - \bar{\sigma}(\mathbf{b}_1 - \bar{\mathbf{b}}_2) - \bar{\sigma}(\mathbf{b}_2 - \bar{\mathbf{b}}_1) \right]
$$
$$
\times \left[\text{Tr}[aabb]\, B^{(1)} + \text{Tr}[abab]\, B^{(2)} \right] \,, \quad (4.40)
$$

where we have introduced the notational shorthands

$$
B^{(1)} = \bar{\sigma}(\mathbf{b}_1 - \bar{\mathbf{b}}_1) + \bar{\sigma}(\mathbf{b}_2 - \bar{\mathbf{b}}_2)
$$
$$
+ \bar{\sigma}(\bar{\mathbf{b}}_1 - \bar{\mathbf{b}}_2) + \bar{\sigma}(\mathbf{b}_2 - \mathbf{b}_1) - 4\, \bar{\sigma}(0) \,, \quad (4.41)
$$
$$
B^{(2)} = \bar{\sigma}(\bar{\mathbf{b}}_1 - \bar{\mathbf{b}}_2) + \bar{\sigma}(\mathbf{b}_1 - \mathbf{b}_2)
$$
$$
- \bar{\sigma}(\mathbf{b}_1 - \bar{\mathbf{b}}_2) - \bar{\sigma}(\mathbf{b}_2 - \mathbf{b}_1) \,. \quad (4.42)
$$

For the cross section (4.40), colour triviality is the condition that $B^{(2)}$ vanishes. However, $B^{(2)} \neq 0$, and colour interference terms remain in (4.40). In contrast, the elastic part of the $N = 2$ photoabsorption cross section is colour trivial since it involves by construction only contact terms. Colour triviality (non-triviality) of the inelastic part of the photoabsorption cross section thus implies automatically the colour triviality (non-triviality) of the corresponding total cross section.

In general, the more inclusive the cross section, the more likely it is colour trivial. In this sense, tagged cross sections are very exclusive since they require detailed knowledge of the final state of the medium. On the other hand, calculating more inclusive observables from (4.40), one recovers colour trivial examples. Especially, the $\mathbf{p}_{2\perp}$-integral (or $\mathbf{p}_{1\perp}$-integral) of (4.40) turns out to be colour trivial. This is expected, of course, since these integrated versions of (4.40) determine the $N = 2$ term of (4.37) in the $\nu \to \infty$-limit.

Based on these results, one may ask whether all one-fold differential photoabsorption cross sections are colour trivial. This is not the case as can be seen e.g. from the inelastic parts of the one-fold differential cross sections

14

$$\frac{d\sigma^{\gamma^*\to q\bar{q}}_{\text{inel.}}}{d\alpha\, d\left(\mathbf{p}_1^\perp - \mathbf{p}_2^\perp\right)}\,, \tag{4.43}$$

$$\frac{d\sigma^{\gamma^*\to q\bar{q}}_{\text{inel.}}}{d\alpha\, d\left(\mathbf{p}_1^\perp + \mathbf{p}_2^\perp\right)}\,. \tag{4.44}$$

For these cross sections, the arguments of $\bar{\sigma}$ in the expression (4.42) for $B^{(2)}$ are constraint by $\mathbf{b}_1 - \bar{\mathbf{b}}_1 = \pm\left(\mathbf{b}_2 - \bar{\mathbf{b}}_2\right)$. It is easy to check that $B^{(2)} \neq 0$, i.e., both results are not colour trivial for $N = 2$ and thus they cannot be colour trivial for $N = $ arbitrary. For a colour trivial expression, it is crucial that (3.9) is not integrated over some average or relative momentum but over the transverse momentum of a final state particle. This is necessary for using the identities of Fig. 7 (a) and (b).

F. Mueller's dipole formulas as eikonal approximation

Explicit calculations of the $p_\perp$-integrated and one-fold differential photoabsorption cross sections (4.24)-(4.26) and (4.37)-(4.40) respectively require an explicit representation of the path integral $\mathcal{K}$. This necessarily involves an approximation. In this section, we study the eikonal approximation which substitutes the path integrals $\mathcal{K}$ by their ultrarelativistic limit

$$\lim_{\nu\to\infty}\mathcal{K}\left(L, \mathbf{r}; 0, \mathbf{b}|\mu\right) = \delta^{(2)}\left(\mathbf{b} - \mathbf{r}\right) S(\mathbf{b})\,. \tag{4.45}$$

We consider a homogeneous density distribution $n(\xi) = n_0$ for a target of longitudinal extension L and we write for the Glauber-type suppression factor

$$S(\mathbf{b}) = e^{-\frac{1}{2}\,n\,L\,\sigma(\mathbf{b})}\,. \tag{4.46}$$

Also, we neglect the phase factors $\exp\{iq\left(\xi - \xi'\right)\}$ in this $\nu \to \infty$-limit, see our discussion of (4.28), (4.29) above. In the ultrarelativistic limit, all photoabsorption cross sections reduce to standard Glauber-type expressions:

$$\lim_{\nu\to\infty}\sigma^{\gamma^*\to q\bar{q}}_{inel.} = N_c\,\alpha_{\text{em}}\int d\alpha\int d\mathbf{b}\,\Phi\left(\mathbf{b}; \mathbf{b}; \alpha\right)$$
$$\times\left[1 - S^2(\mathbf{b})\right]\,, \tag{4.47}$$

$$\lim_{\nu\to\infty}\sigma^{\gamma^*\to q\bar{q}}_{diff.} = N_c\,\alpha_{\text{em}}\int d\alpha\int d\mathbf{b}\,\Phi\left(\mathbf{b}; \mathbf{b}; \alpha\right)$$
$$\times\left[1 - S(\mathbf{b})\right]^2\,, \tag{4.48}$$

$$\lim_{\nu\to\infty}\sigma^{\gamma^*\to q\bar{q}}_{total} = 2\,N_c\,\alpha_{\text{em}}\int d\alpha\int d\mathbf{b}\,\Phi\left(\mathbf{b}; \mathbf{b}; \alpha\right)$$
$$\times\left[1 - S(\mathbf{b})\right]\,. \tag{4.49}$$

This total photoabsorption cross section is Mueller's dipole formula first derived in Ref. [4]. Also, the elastic cross section is known to describe the diffractive contribution to the deep inelastic scattering structure function F_2 in the ultrarelativistic limit [8].

The one-fold differential cross sections read in the eikonal limit

$$\lim_{\nu\to\infty}\frac{d\sigma^{\gamma^*\to q\bar{q}}_{\text{inel.}}}{d\alpha\, d\mathbf{p}_1^\perp} = \frac{\alpha_{\text{em}}\,N_c}{(2\pi)^2}\int d\mathbf{b}\, d\bar{\mathbf{b}}\,\Phi(\mathbf{b}; \bar{\mathbf{b}}; \alpha)e^{i\,\mathbf{p}_1^\perp\cdot(\mathbf{b}-\bar{\mathbf{b}})}$$
$$\times\left[S(\mathbf{b} - \bar{\mathbf{b}}) - S(\bar{\mathbf{b}})\,S(\mathbf{b})\right]\,, \tag{4.50}$$

$$\lim_{\nu\to\infty}\frac{d\sigma^{\gamma^*\to q\bar{q}}_{\text{diff.}}}{d\alpha\, d\mathbf{p}_1^\perp} = \frac{\alpha_{\text{em}}\,N_c}{(2\pi)^2}\int d\mathbf{b}\, d\bar{\mathbf{b}}\,\Phi(\mathbf{b}; \bar{\mathbf{b}}; \alpha)e^{i\,\mathbf{p}_1^\perp\cdot(\mathbf{b}-\bar{\mathbf{b}})}$$
$$\times\left[1 - S(\bar{\mathbf{b}})\right]\left[1 - S(\mathbf{b})\right]\,, \tag{4.51}$$

$$\lim_{\nu\to\infty}\frac{d\sigma^{\gamma^*\to q\bar{q}}_{\text{total}}}{d\alpha\, d\mathbf{p}_1^\perp} = \frac{\alpha_{\text{em}}\,N_c}{(2\pi)^2}\int d\mathbf{b}\, d\bar{\mathbf{b}}\,\Phi(\mathbf{b}; \bar{\mathbf{b}}; \alpha)e^{i\,\mathbf{p}_1^\perp\cdot(\mathbf{b}-\bar{\mathbf{b}})}$$
$$\times\left[1 + S(\mathbf{b} - \bar{\mathbf{b}}) - S(\bar{\mathbf{b}}) - S(\mathbf{b})\right]\,. \tag{4.52}$$

The elastic contribution (4.51) has been obtained previously in calculations of the diffractive component of DIS electron nucleon scattering with one resolved jet in the final state [8]. Furthermore, the total cross section (4.52) was previously obtained by Mueller (see eq. (27) of Ref. [7]) from a one-loop calculation arguing then for its general validity. In passing, we recall Mueller's interpretation of the four terms in (4.52): for the case $p_1^{\perp\,2} \ll Q^2$, the first two terms turn out to be of equal size while the last two terms are negligible [7]. Looking at the diagrammatic contributions one concludes that in this limit the term proportional $S(\mathbf{b} - \bar{\mathbf{b}})$ gives the probability that a quark which gets many random kicks is found with relatively small transverse momentum. The term proportional to 1, on the other hand, corresponds to the case of no scattering and can be viewed as the quantum mechanical shadow of the term proportional to $S(\mathbf{b}-\bar{\mathbf{b}})$ [7].

G. Corrections to the eikonal approximation

To go beyond the eikonal limit, we discuss now the Gaussian dipole approximation for the path-integrals $\mathcal{K}$. It is based on the observation that the main support in the path integral (4.19) comes from small transverse distances $r = |\mathbf{r}|$, where the cross section $\sigma(\mathbf{r})$ in (4.8) has a leading quadratic dependence:

$$\sigma(\mathbf{r}) \approx C(r)\,r^2\,. \tag{4.53}$$

In explicit model calculations, one finds [14,21] that the r-dependence of $C(r)$ is a slow logarithmic one, and can be neglected. For the dipole cross section in (4.8), an expansion to order r^2 confirms this feature. One finds

$$C = \frac{C_F}{2}\int^{\kappa_c}\frac{d^2\boldsymbol{\kappa}_\perp}{(2\pi)^2}\,\boldsymbol{\kappa}_\perp^2\,|a_0(\boldsymbol{\kappa}_\perp)|^2\,, \tag{4.54}$$

where the $\boldsymbol{\kappa}_\perp$-integral depends logarithmically on the ultraviolet cut-off κ_c which one has to introduce in this approximation. We note that C provides a measure of the average transverse momentum transfer $\langle\boldsymbol{\kappa}_\perp^2\rangle$ in

a single scattering. For sufficiently small r, when the r-dependence of C can be neglected, the path integral (4.19) reduces to that of a harmonic oscillator [14]

$$\mathcal{K}_{\mathrm{osz}}\big(\mathbf{r}_2, L; \mathbf{r}_1, 0|\mu\big) = \frac{A}{\pi\, i}\exp\big\{iAB(\mathbf{r}_1^2 + \mathbf{r}_2^2)$$
$$-2\,i\,A\,\mathbf{r}_1 \cdot \mathbf{r}_2\big\}\,, \qquad (4.55)$$

$$A = \frac{\mu\Omega}{2\,\sin(\Omega\,L)}\,, \qquad (4.56)$$

$$B = \cos(\Omega\,L)\,, \qquad (4.57)$$

with the oscillator frequency

$$\Omega = \frac{1 - i}{\sqrt{2}}\sqrt{\frac{n_0\,C}{\mu}}\,. \qquad (4.58)$$

For what follows, it is important that the $\mu \to \infty$-limit of $\mathcal{K}_{\mathrm{osz}}$ coincides with the eikonal limit (4.45) of the unapproximated path-integral. To see this, we expand the norm of $\mathcal{K}_{\mathrm{osz}}$ to leading order in μ and the phase to next to leading order,

$$\mathcal{K}_{\mathrm{osz}}\big(\mathbf{r}_2, L; \mathbf{r}_1, 0|\mu\big) = \frac{\mu + O\left(\mu^0\right)}{2\pi\, i\, L}\,\exp\left\{\frac{i\mu}{2L}\,(\mathbf{r}_e - \mathbf{r})^2\right.$$
$$\left. -\frac{Ln_0C}{6}\left[\mathbf{r}_e^2 + \mathbf{r}^2 + \mathbf{r}_e\cdot\mathbf{r}\right] + O\left(\mu^{-1}\right)\right\}$$
$$\overset{\mu\to\infty}{\longrightarrow} \quad \delta^{(2)}\left(\mathbf{r}_e - \mathbf{r}\right)\,e^{-\frac{1}{2}\,n_0\,L\,C\,\mathbf{r}^2}\,, \qquad (4.59)$$

which coincides with (4.45) for the quadratic ansatz $\sigma\left(\mathbf{r}\right) = C\,\mathbf{r}^2$. The harmonic oscillator approximation thus provides an explicit representation for the path-integral $\mathcal{K}$ which preserves the correct high energy limit. At least numerically, this allows for an explicit study of the $1/\mu$-corrections to the eikonal limit of the cross sections (4.24)-(4.26) and (4.37)-(4.39). To explore some qualitative features of these $1/\mu$-corrections analytically, we take here recourse to a Gaussian approximation Φ_G of the incoming Born wavefunction:

$$\Phi_G(\mathbf{r}, \bar{\mathbf{r}}; \alpha) = \psi(\mathbf{r})\,\psi^*(\bar{\mathbf{r}})\,, \qquad (4.60)$$
$$\psi(\mathbf{r}) = \frac{1}{\pi\,R^2}\exp\left(-\mathbf{r}^2/R^2\right)\,, \qquad (4.61)$$
$$\frac{1}{R^2} = (1 - \alpha)\alpha Q^2 + m^2\,, \qquad (4.62)$$

where the radius R is chosen to reproduce the characteristic width of the fall-off of the exact Born probability Φ given in (B8) and (B14).

The time-evolved final state wavefunction reads

$$\Psi_f(\bar{\mathbf{r}}) = \int d\mathbf{r}\,\mathcal{K}_{\mathrm{osz}}(\bar{\mathbf{r}}, L; \mathbf{r}, 0|\mu)\,\psi(\mathbf{r})$$
$$= \frac{1 + O(\mu^{-1})}{\pi\,R^2}\exp\left[-\frac{\bar{\mathbf{r}}^2}{R^2} - \frac{1}{2}n_0\,L\,C\,\bar{\mathbf{r}}^2 + i\,q\,L\right.$$
$$\left. i\frac{\bar{\mathbf{r}}^2}{\mu}\,c_1 - \frac{\bar{\mathbf{r}}^2}{\mu^2}\,c_2 + O(\mu^{-3})\right]\,. \qquad (4.63)$$

Here, we have used the phase convention (4.27) to obtain the term $i\,q\,L$ in the exponent. The shorthands c_1 and c_2 denote the leading real and imaginary $1/\mu$-corrections to the final state wavefunction:

$$c_1 = \frac{L}{6}\left[n_0^2L^2C^2 + 6\frac{n_0LC}{R^2} + \frac{12}{R^4}\right]\,, \qquad (4.64)$$

$$c_2 = \frac{L^2}{15}\left[n_0^3L^3C^3 + 10\frac{n_0^2L^2C^2}{R^2} + 40\frac{n_0LC}{R^4} + \frac{60}{R^6}\right]\,. \qquad (4.65)$$

Deviations from the eikonal limit can be calculated with the help of (4.63). For example, we find for the total photoabsorption cross section (4.26):

$$\sigma_{\mathrm{total}}^{\gamma^* \to q\bar{q}} - \lim_{\nu\to\infty}\sigma_{\mathrm{total}}^{\gamma^* \to q\bar{q}}$$
$$= N_c\,\alpha_{\mathrm{em}}\int d\alpha\int d\mathbf{r}\,\Phi_G(\mathbf{r}, \mathbf{r}; \alpha)\,S(\mathbf{r})$$
$$\times 2\left[1 - e^{-\mathbf{r}^2c_2/\mu^2}\cos\left(\frac{\mathbf{r}^2}{\mu}c_1 + q\,L\right)\right]\,. \qquad (4.66)$$

In the $\nu \to \infty$-limit, this difference vanishes by construction. To understand which scales determine the deviations from the eikonal limit, we recall that $1/(\mu\,R^2) = q$ has an interpretation as inverse coherence length $1/l_f$ and n_0LC is the total transverse momentum squared accumulated during the rescattering over a distance L. The eikonal approximation is thus justified if the phases determined by the coherence length and the total transverse energy $E_\perp^{\mathrm{tot}}$ are negligible:

$$q\,L \ll 1\,, \qquad (4.67)$$
$$E_\perp^{\mathrm{tot}}\,L = \frac{n_0LC}{2\mu}\,L \ll 1\,. \qquad (4.68)$$

We conclude this section with two technical remarks:

1. The explicit form of the incoming q-$\bar{q}$ wavefunctions (B6), (B13) is given in terms of the Bessel function K_0 which has an integral representation in terms of a Gaussian in $\mathbf{r}$,

$$K_0(\epsilon\,|\mathbf{r}|) = \frac{1}{2}\int_{-\infty}^{0}\frac{dy_L}{y_L}\,e^{-i\frac{\epsilon^2}{4\,y_L}\mathbf{r}^2 + i\,y_L}\,. \qquad (4.69)$$

The evolution of the Gaussian wavefunction $\psi(\mathbf{r})$ in (4.63) can thus be used for the exact calculation if $1/R^2$ is taken to be the width $\frac{\epsilon^2}{4\,y_L}$ of the integrand of (4.69) and the y_L-integration is done afterwards. However, to order $1/\mu$, terms proportional to $1/R^4$ appear in (4.63) and thus the y_L-integration cannot be done analytically if $1/\mu$-corrections are included. Only the $\mu \to \infty$-limit can be accessed analytically in this way.

2. A surprising difficulty occurs in the calculation of the photoabsorption cross section (4.24) from the harmonic oscillator approximation (4.55) if one tries to do the $\mathbf{r}_e$-integration first:

$$F_{\text{osz}}(\bar{\mathbf{r}}, \mathbf{r}) = \int d\mathbf{r}_e \, \mathcal{K}_{\text{osz}}(\bar{\mathbf{r}}, 0; \mathbf{r}_e, L|\mu) \, \mathcal{K}_{\text{osz}}(\mathbf{r}_e, L; \mathbf{r}, 0|\mu) \,.$$

$$(4.70)$$

After a lengthy but straightforward calculation, we find for the $\mu \to \infty$-limit

$$\lim_{\mu \to \infty} F_{\text{osz}}(\bar{\mathbf{r}}, \mathbf{r}) = \delta^{(2)}(\bar{\mathbf{r}} - \mathbf{r}) \, e^{-\frac{1}{4} n_0 L C \mathbf{r}^2} \,, \qquad (4.71)$$

whose exponent differs from that of the eikonal dipole formula (4.45) by a factor $\frac{1}{4}$. This mismatch is an artefact stemming from a calculation which performs simplifications on the cross section level before completing the dynamical evolution on the amplitude level. Starting from (4.63) for $\Psi_f(\mathbf{r}_e)$ and calculating $\Psi_f(\mathbf{r}_e) \, \Psi_f^*(\mathbf{r}_e)$, one obviously reproduces for (4.24) the eikonal expression (4.47) in the $\mu \to \infty$-limit.

V. PHOTODISSOCIATION VIA NON-ABELIAN STOKES'S THEOREM

In this section, we argue that the dipole cross section (4.8) parametrizes the transverse components of the chromoelectric field strength correlations $\langle F F \rangle$ in the nuclear medium. This suggests an interpretation of $\sigma(\mathbf{r})$ which holds model-independent, i.e., irrespective of whether we have build up (4.8) from the model ansatz (2.10), or from some other model parametrization of the colour target field.

We first recall the non-abelian Stokes's theorem. This relates the integral of the non-abelian vector potential A_μ along a closed contour C to the area integral of the field strength tensor $F^{\mu\nu}$, [33-35]

$$\text{Tr} \, \mathcal{P} \exp \left(\oint_C dz_\mu \, A^\mu(z) \right)$$
$$= \text{Tr} \, \mathcal{P}_{\text{area}} \exp \left(\int d\sigma_{\mu\nu}(y) \, U_{Ay} \, F^{\mu\nu}(y) \, U_{yA} \right) \,. \qquad (5.1)$$

Here, the U_{Ay} are parallel transporters. They ensure that the r.h.s. is gauge-invariant. Equation (5.1) does not depend on the choice of the position A, since cyclicity of the trace allows to change the reference point by substituting $U_{Ay} \to U_{BA} U_{Ay}$. The area ordering $\mathcal{P}_{\text{area}}$ is defined by disecting the area enclosed by C in many (ultimately: infinitessimally small) areas in such an order that the parallel transporters C_i along the infinitesimal areas combine to C. As a consequence of the non-Abelian Gauss theorem, (5.1) turns out to be independent of the orientation of the surface $d\sigma_{\mu\nu}(y)$ [35].

The total photoabsorption cross section (4.1) is closely related to the Stokes's theorem, as can be seen from the representation

$$\sigma_{total}^{\gamma^* \to q \bar{q}} = \alpha_{\text{em}} \int d\alpha \int d\mathbf{b}_1 \, d\mathbf{b}_2 \, d\bar{\mathbf{b}}_1 \, d\bar{\mathbf{b}}_2 \, \Phi(\Delta \mathbf{b}; \Delta \bar{\mathbf{b}}; \alpha)$$

$$\times \int \mathcal{D} r_1 \, \mathcal{D} r_2 \, e^{\frac{i\nu}{2} \int \left(\alpha \dot{r}_2^2 + (1-\alpha) \dot{r}_1^2 \right)}$$

$$\times \int \mathcal{D} \bar{r}_1 \, \mathcal{D} \bar{r}_2 \, e^{\frac{i\nu}{2} \int \left(-\alpha \dot{\bar{r}}_2^2 - (1-\alpha) \dot{\bar{r}}_1^2 \right)}$$

$$\times \left\langle \text{Tr} \, \mathcal{P} \exp \left(\oint_{C(r_1, r_2, \bar{r}_1, \bar{r}_2)} dz_\mu \, A^\mu(z) \right) \right\rangle \quad (5.2)$$

Here, C is defined by the transverse paths $\mathbf{r}_1(\xi)$, $\bar{\mathbf{r}}_1(\xi)$, $\mathbf{r}_2(\xi)$, $\bar{\mathbf{r}}_2(\xi)$ which denote the positions of the rescattering quark and anti-quark in the path integral representation (2.17) of the corresponding Green's functions. We can consider C as a closed path since we work for a static potential $A_\mu = \delta_{\mu 0} A_0$ for which the Wilson line along purely transverse directions $d\mathbf{x}_\perp A_\perp(x)$ vanishes. The photoabsorption cross section (5.2) is thus given by a closed Wilson loop which sums up the gluon field strength of the medium in the area determined by the paths of the rescattering q- and $\bar{q}$- quarks.

The connection between total hadronic cross sections as (5.2) and closed Wilson loops has been studied extensively, see e.g. [25,37]. Phenomenological applications of the non-abelian Stokes's theorem (5.1) were pioneered by Dosch and coauthors [36,37]. In Dosch's approach, one takes recourse to an axial gauge in which the parallel transporters on the r.h.s. of (5.1) reduce to unit operators. The remaining expression is then expanded in powers of F. Our discussion of (5.2) borrows from this strategy. Clearly, we cannot choose an axial gauge to remove the parallel transporters in (5.1), since our gauge freedom is already exhausted by the definition (2.10). However, we can invoke the proof of colour triviality of (5.2) to discuss the equivalent abelian problem with a rescaled vector potential $A_\mu \to \sqrt{C_F} A_\mu$. We find

$$\left\langle \exp \left(-i g \sqrt{C_F} \oint_C ds \, A^\mu(\omega_s) \frac{\partial \omega_s^\mu}{\partial s} \right) \right\rangle$$

$$= \left\langle \exp \left(i g \sqrt{C_F} \int_S F_{\mu\nu}(\omega_s) \frac{\partial \omega_s^\mu}{\partial s} \frac{\partial \omega_s^\nu}{\partial x_\alpha} ds \, dx_\alpha \right) \right\rangle$$

$$= \left\langle \exp \left(-i g \sqrt{C_F} \int_{z_1}^{z_2} d\xi \int_{\mathbf{r}_1(\xi)}^{\mathbf{r}_2(\xi)} dx_\perp^i \, E_i^\perp(\mathbf{x}_\perp, \xi) \right) \right\rangle$$

$$= 1 - \int_{z_1}^{z_2} d\xi \, n(\xi) \frac{g^2 C_F}{2} \left\langle \int d\bar{\xi} \int_{\mathbf{r}_1(\xi)}^{\mathbf{r}_2(\xi)} dx_\perp^i \, dx_\perp'^j \right.$$

$$\left. \times E_i^\perp(\mathbf{x}_\perp, \xi) \, E_j^\perp(\mathbf{x'}_\perp, \xi + \bar{\xi}) \right\rangle + O(n^2(\xi)) \,. \quad (5.3)$$

Here, ω_s^μ denotes the path around the contour C, and the notation is specified in Fig. 11.
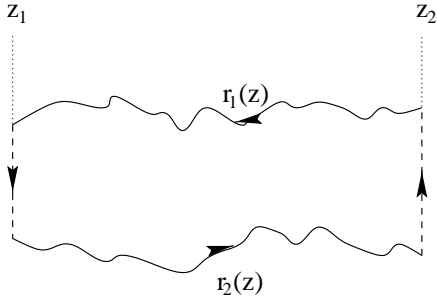
FIG. 11. The closed Wilson loop between longitudinal positions z_1 and z_2, as considered in (5.3).

We have used the particular form of a static colour potential $A_\mu = \delta_{\mu 0} A_0$ to rewrite the r.h.s. of (5.1) in terms of transverse electric fields. The detailed arguments for the shift of integration variables needed to arrive at the last equation of (5.3) are given in appendix B of Ref. [21]. The same appendix contains the derivation of the dipole cross section (4.8) from a closed abelian Wilson loop:

$$
\left\langle \exp\left(-i\, g\, \sqrt{C_F} \oint_C ds\, A^\mu(\omega_s)\, \frac{\partial \omega_s^\mu}{\partial s} \right) \right\rangle =
$$
$$
\left\langle \exp\left(-i\, g\, \sqrt{C_F} \int_{z_1}^{z_2} d\xi\, [A_0(\mathbf{r}_1(\xi),\xi) - A_0(\mathbf{r}_2(\xi),\xi)] \right) \right\rangle
$$
$$
= \exp\left(- \int_{z_1}^{z_2} d\xi\, n(\xi)\, \sigma\left(\mathbf{r}_1(\xi) - \mathbf{r}_2(\xi)\right) \right). \qquad (5.4)
$$

Comparing (5.4) to (5.3), we can relate the dipole cross section to the two-point correlation function of the transverse electric field strength,

$$
\sigma\left(\mathbf{r}_1(\xi) - \mathbf{r}_2(\xi)\right) = \left\langle \int d\bar{\xi} \int_{\mathbf{r}_1(\xi)}^{\mathbf{r}_2(\xi)} dx_\perp^i \, dx_\perp'^j \right.
$$
$$
\left. \times E_i^\perp(\mathbf{x}_\perp,\xi)\, E_j^\perp(\mathbf{x'}_\perp, \xi + \bar{\xi}) \right\rangle. \qquad (5.5)
$$

As long as we parametrize this dipole cross section by the Gaussian approximation $\sigma(\mathbf{r}) = C\, r^2$, only the average of the colour field strength enters our final results in form of one single parameter C. The final result is model-independent in the sense that it does not depend on the model-specific way in which the colour field strength giving rise to C was modelled.

VI. CONCLUSION

Colour triviality provides a crucial simplification of an otherwise untractable problem. In general, the N-fold rescattering of a parton in a colour target field leads in the cross section to colour traces over $2N$ generators. For sufficiently exclusive processes, the huge number of colour interference terms thus limits explicit calculations of the soft nuclear dependence of hard partonic processes to the case of very few rescatterings [23]. Colour triviality is

the consequence of a complete diagrammatic cancellation between these different colour interference terms. For colour trivial observables, all non-abelian complications reduce to the rescaling of coupling constants by appropriate powers of Casimirs. The multiple scattering problem thus becomes an abelian one. The soft nuclear dependence of hard colour-trivial observables can be described in terms of a QCD dipole cross section which absorbs the leading medium-dependence in a one-parameter estimate C of the average target colour field strength. This makes the identification of colour-trivial observables of particular interest for relativistic heavy ion collisions at RHIC and LHC where very little is known about the medium a priori but many "hard probes" are expected to receive sizeable nuclear modifications due to rescattering effects.

In the present work, we have derived an explicit general expression for the rescattering effects on a hard coloured parton inside a spatially extended nuclear medium. We have then studied in detail for the simple example of virtual photodissociation under which conditions this general rescattering formula results in colour-trivial observables which can be parametrized by a QCD dipole cross section. In detail:

The non-abelian Furry wavefunction (2.12) derived in section II is a high-energy approximation to the solution of the non-abelian Dirac equation in a spatially extended colour field. In contrast to other approximate solutions [28], it is accurate up to order $O(1/E^2)$ in the phase. This is known to be indespensable for calculating the nuclear dependence of observables which are determined by the destructive interference between different production amplitudes as e.g. the LPM-effect or the nuclear dependence of Drell-Yan yields. The Furry wavefunction (2.12) thus provides a unified starting point for the description of the nuclear dependence of a large class of observables.

Based on the Green's function $\bar{G}$ which describes the dynamical evolution of the non-abelian Furry wavefunction, we have derived in section IV a set of diagrammatic identities which play the key role in proofs of colour triviality. These identities exploit the integration over the transverse momentum of a single final state particle only. They are thus much stronger than diagrammatic cancellations implied by the optical theorem. As a consequence, they ensure for the example of the $\gamma^* \to q\bar{q}$ process a colour trivial result not only for the total, elastic and inelastic inclusive photoabsorption cross section but also for cases in which one jet is resolved in the final state. All these observables can be described in terms of the same one-parameter QCD dipole cross section.

Earlier applications of these diagrammatic techniques as well as statements about the colour triviality of the photoabsorption cross section exist [4,15-18,27,7,8]. Here, we have given relatively short and complete proofs of these statements by exploiting the advantages of a new and compact configuration-space notation implied by the

Furry wavefunction. In contrast to previous discussions, our formulation includes the transverse dynamical evolution of the partons. For the example of the photoabsorption cross section studied here, this allowed us to quantify the leading deviations from the eikonal limit which grow at fixed energy proportional to L^2. Moreover, the compactness of our notation made it possible to discuss in detail technically rather involved processes as e.g. the inelastic and total photoabsorption cross section with one jet resolved in the final state. This points to the strength of the present approach which we believe to be suited for the explicit discussion of more complicated processes as, e.g., further studies of the transverse momentum dependence of the non-abelian LPM-effect [17,21] or photodissociation including initial state gluon radiation [32].

ACKNOWLEDGMENTS

APPENDIX A: NON-ABELIAN FURRY APPROXIMATION

In this appendix, we derive the non-abelian Furry wavefunction (2.12) from the set of N-scattering Feynman diagrams (2.11). For an N-fold rescattering diagram, we use the notation $\mathbf{p}_{N+1} \equiv \mathbf{p}$ for the final state momentum. To simplify $I^{(N)}(\mathbf{y})$ in (2.11), we do the longitudinal momentum integrals by contour integration

$$
\int \frac{dp_i^L}{(2\pi)} \frac{i\,(\not{p}_i + m)\,\gamma_0}{p_i^2 - m^2 + i\,\epsilon}\, e^{i\,p_i^L\,(x_i^L - x_{i-1}^L)}
$$
$$
= \frac{(\not{p}_i + m)\,\gamma_0}{2\,p_i^L}\Theta(x_i^L - x_{i-1}^L)\, e^{i\,p_i^L\,(x_i^L - x_{i-1}^L)}\,. \quad \text{(A1)}
$$

We note that, strictly speaking, the position variables x_i in this expression are integration variables and do not coincide with the center of the i-th scattering potential.

A more detailed analysis of (2.11) involves for a particular model also the study of the p_i^L-poles of the Fourier-transformed single scattering potentials. For a Yukawa-type potential $1/[(\mathbf{p}_i - \mathbf{p}_{i-1})^2 + M^2]$, e.g., these poles give additional contributions to the p_i^L-integrals, which are however exponentially suppressed due to the Debye-screening mass M. These details are discussed explicitly in Refs. [12,15] and for contact terms in Ref. [38]. In the end, the only $O(1/E)$-contribution to the p_i^L-integration turns out to be given by (A1). On the r.h.s. of this equation, p_i^L is determined by the pole value to order $O(1/E)$, $p_i^L = p - \frac{p_i^{\perp\,2}}{2\,p}$ where $p^2 = E^2 - m^2$. Using $\mathbf{x}_0 \equiv \mathbf{y}$, we can rewrite (2.11) as

$$
I^{(N)}(\mathbf{y}) = e^{-i\,p\,y_L}\,\mathcal{P}\,\left(\prod_{i=1}^{N} \int \frac{d^2\mathbf{p}_i^{\perp}}{(2\pi)^2}\, d^3\mathbf{x}_i\,\Theta(x_i^L - x_{i-1}^L)\right.
$$
$$
\times \frac{(\not{p}_i + m)\,\gamma_0}{2\,p_i^L}\,[-i\,A_0(\mathbf{x}_i)]\, e^{i\,\mathbf{p}_i^{\perp}\cdot(\mathbf{x}_i^{\perp} - \mathbf{x}_{i-1}^{\perp})}
$$
$$
\left.\times e^{-i\frac{p_i^{\perp\,2}}{2\,p}(x_i^L - x_{i-1}^L)}\right)\, e^{-i\mathbf{p}\cdot\mathbf{x}_N + i\,p\,x_N^L}\, v^{(r)}(\mathbf{p})\,. \quad \text{(A2)}
$$

We now consider the spinor structure of this expression. To order $O(1/E^2)$, each quark propagator introduces a numerator

$$
(\not{p}_i + m)\gamma_0 \approx E(\gamma_0 - \gamma_3)\gamma_0 - \gamma^{\perp}\cdot\mathbf{p}_i^{\perp}\,\gamma_0 + \gamma_3\,\gamma_0\,\frac{p_i^{\perp\,2}}{2\,p}\,. \quad \text{(A3)}
$$

The normalization of $I^{(N)}(\mathbf{y})$ is needed to leading order in energy only. This allows us to neglect the mass term in (A3). For the same reason, it is sufficient to keep only the leading term $E(\gamma_0 - \gamma_3)\gamma_0$ for all numerators (A3) with $i \geq 2$. Further simplification of (A2) is then possible, using

$$
(E(\gamma_0 - \gamma_3)\gamma_0)^n = 2^{n-1}\,E^n\,(\gamma_0 - \gamma_3)\gamma_0\,. \quad \text{(A4)}
$$

The case $i = 1$ is different: depending on the explicit form of the production vertex, the leading order contribution of this numerator can cancel. We have to keep the numerator $(\not{p}_1 + m)\gamma_0$ to order $O(1/E)$. To this aim, we substitute in (A2)

$$
(\not{p}_1 + m)\gamma_0 \longrightarrow E(\gamma_0 - \gamma_3)\gamma_0 - i\gamma\cdot\frac{\partial}{\partial\mathbf{y}}\gamma_0\,, \quad \text{(A5)}
$$

where the differential operator acts on the big bracket in (A2). Equation (A5) is equivalent to (A3) with the transverse components written in configuration space. In a coordinate system with $\mathbf{p} \parallel \mathbf{n}$, the above equation takes the form

$$
\not{p}_1\gamma_0 = p(\gamma_0 - \gamma_3)\gamma_0 + \boldsymbol{\alpha}^{\perp}\cdot(\mathbf{p}_1^{\perp} - \mathbf{p}^{\perp})
$$
$$
- \alpha^L\left(\frac{\mathbf{p}_1^{\perp\,2}}{2\,p} - \frac{\mathbf{p}^{\perp\,2}}{2\,p}\right)
$$
$$
\longrightarrow \quad p\,(\gamma_0 - \gamma_3)\gamma_0 + i\boldsymbol{\alpha}\cdot\frac{\partial}{\partial\mathbf{y}} - \boldsymbol{\alpha}\cdot(\mathbf{p} - p\,\mathbf{n})\,. \quad \text{(A6)}
$$

In the same coordinate system, $0.5\,(1-\gamma_3\gamma_0)\,v(\mathbf{p}) = v(\mathbf{p})$. Acting with (A6) on $v(\mathbf{p})$, we thus find to leading order in E an expression proportional to $\hat{D}\,v(\mathbf{p})$. With these steps, the amplitude (A2) takes the form

$$
I^{(N)}(\mathbf{y}) = e^{-i\,p\,y_L}\,\hat{D}\,\mathcal{P}\int\left(\prod_{i=1}^{N} d^3\mathbf{x}_i\,\Theta(x_i^L - x_{i-1}^L)\right)
$$
$$
\times\left(\prod_{i=1}^{N}[-i\,A_0(\mathbf{x}_i)]\,\bar{G}_0(\mathbf{x}_{i-1},\mathbf{x}_i|p)\right)\int d\mathbf{x}_\perp
$$
$$
\times\bar{G}_0(\mathbf{x}_N,\mathbf{x}|p)F(\mathbf{x}_\perp,x^L,\mathbf{p})\,v^{(r)}(p)\,. \qquad (A7)
$$

Here, we have introduced two elements of the abelian Furry approximation: the outgoing transverse plane wave F and the free Green's function $\bar{G}_0$ of (2.15) which we have identified here with the Gaussian $\mathbf{p}_i^\perp$-integrals,

$$
\bar{G}_0(\mathbf{x}_{i-1}^\perp, x_{i-1}^L; \mathbf{x}_i^\perp, x_i^L|p)
$$
$$
= \int\frac{d^2\mathbf{p}_i^\perp}{(2\pi)^2}\,e^{i\,\mathbf{p}_i^\perp\cdot(\mathbf{x}_i^\perp - \mathbf{x}_{i-1}^\perp)}\,e^{-i\frac{p_i^{\perp\,2}}{2\,p}(x_i^L - x_{i-1}^L)}\,. \qquad (A8)
$$

For the path-ordered product in (A7) which involves these Green's functions, we introduce the shorthand

$$
\bar{G}^{(N)}(\mathbf{y}_\perp, y_L; \mathbf{x}_\perp, x_L|p) =
$$
$$
\mathcal{P}\left(\prod_{i=1}^{N+1}\int d^3\mathbf{x}_i\,\Theta(x_{i+1}^L - x_i^L)\right)\bar{G}_0(\mathbf{y}_\perp, y_L; \mathbf{x}_1^\perp, x_1^L|p)
$$
$$
\times\left(\prod_{i=1}^{N+1}[-i\,A_0(\mathbf{x}_i)]\,\bar{G}_0(\mathbf{x}_i^\perp, x_i^L; \mathbf{x}_{i+1}^\perp, x_{i+1}^L|p)\right)\,, \qquad (A9)
$$

where $\mathbf{x}_{N+1} = \mathbf{x}_\infty$. Allowing for arbitrary many gluon exchanges, we have to sum over N.

$$
\bar{G}(\mathbf{y}_\perp, y_L; \mathbf{x}_\perp, x_L|p) = \sum_{N=0}^{\infty}\bar{G}^{(N)}(\mathbf{y}_\perp, y_L; \mathbf{x}_\perp, x_L|p)\,. \qquad (A10)
$$

From this one sees easily that $G^{(N)}$ corresponds exactly to the N-th order $O(A_0^N)$ term in (2.14). The sum (2.12) over N-fold scattering diagrams takes the form of a non-abelian extension of the Furry approximation.

We emphasize that the approximations used in our derivation and especially the different treatment of the quark propagators at the production vertex and in the final state rescattering part of the amplitude $I^{(N)}$ leads to a consistent high energy expansion with a norm accurate to leading order in $O(1/E)$ and a phase factor accurate up to order $O(1/E^2)$. The same approximation were employed in recent calculations of rescattering amplitudes for which the production vertex P is a photon or gluon emission vertex [12,26].

APPENDIX B: $Q\bar{Q}$ FOCK STATES

In this appendix, we give details of the derivation of transverse and longitudinal components of the squared incoming Fock state

$$
\Phi(\Delta\mathbf{b}; \Delta\bar{\mathbf{b}}; \alpha) = \Phi_\perp(\Delta\mathbf{b}; \Delta\bar{\mathbf{b}}; \alpha) + \Phi_L(\Delta\mathbf{b}; \Delta\bar{\mathbf{b}}; \alpha)\,. \qquad (B1)
$$

We start with the longitudinal polarization ϵ_μ^L, satisfying $\epsilon^L\cdot k = 0$ and $\epsilon^{L\,2} = 1$,

$$
\epsilon_\mu^L = \frac{1}{Q}\left(\sqrt{\nu^2 + Q^2}, \mathbf{0}_\perp, \nu\right)\,. \qquad (B2)
$$

The corresponding vertex function reads to leading order in energy

$$
\Gamma^L = \epsilon_\mu^L\,\hat{\Gamma}^\mu = Q\,\sqrt{(1-\alpha)\,\alpha}\,r\,\delta_{r,r'}\,, \qquad (B3)
$$

where r, r' are the helicities of the quark and antiquark. The square of this longitudinal vertex function, summed over the spin of the final state particles, reads

$$
\sum_{r,r'}\Gamma^L\,\Gamma^{L^*} = 2\,Q^2\,(1-\alpha)\,\alpha\,. \qquad (B4)
$$

This is a kinematical prefactor which factorizes in the integrand of (3.7). For the first interaction in the photodissociation amplitude in (3.7), we take some longitudinal position z_a. The $\mathbf{y}$-integration in (3.7) can then be done analytically. We find

$$
I_L(\mathbf{b}_2 - \mathbf{b}_1|y_L, z_a)
$$
$$
= \int d^2\mathbf{y}_\perp\,\bar{G}_0(\mathbf{b}_2, z_a; \mathbf{y}|p_2)\,\bar{G}_0(\mathbf{y}; \mathbf{b}_1, z_a|p_1)
$$
$$
= \frac{\mu}{2\pi\,i\,(z_a - y_L)}\,\exp\left\{\frac{i\mu\,(\mathbf{b}_2 - \mathbf{b}_1)^2}{2\,(z_a - y_L)}\right\}\,, \qquad (B5)
$$

where $\mu = (1-\alpha)\alpha\,\nu$. The virtual photon has to dissociate at longitudinal position $y_L < z_a$ in order to make an interaction at z_a possible. This limits the range of the y_L-integral:

$$
I_L(\Delta\mathbf{b}|z_a) = \int_{-\infty}^{z_a} dy_L\,I_L(\mathbf{b}_2 - \mathbf{b}_1|y_L, z_a)
$$
$$
= \frac{(1-\alpha)\,\alpha\,\nu}{2\pi\,i}\,e^{i\,q\,z_a}\,2\,K_0(\bar{\epsilon}\,|\Delta\mathbf{b}|)\,, \qquad (B6)
$$
$$
\bar{\epsilon} = \sqrt{(1-\alpha)\alpha\,Q^2 + m^2}\,. \qquad (B7)
$$

If the first interaction occurs at z_a in both the amplitude and complex conjugate amplitude, then the square of the incoming longitudinal $q\bar{q}$ Fock wavefunction is defined as the combination of the squared emission vertex (B4) and the free time evolution (B5),

$$\Phi_L(\Delta\mathbf{b};\Delta\bar{\mathbf{b}};\alpha) = \frac{\sum_{r,r'}\Gamma^L\,\Gamma^{L^*}}{4\nu^2\alpha(1-\alpha)}I_L(\Delta\mathbf{b}|z_a)\,I_L^*(\Delta\bar{\mathbf{b}}|z_a)$$

$$= \frac{Q^2\,\alpha^2\,(1-\alpha)^2}{2\,(2\pi)^2}\,4\,K_0(\bar\epsilon|\Delta\mathbf{b}|)\,K_0(\bar\epsilon|\Delta\bar{\mathbf{b}}|)\,. \qquad \text{(B8)}$$

This expression appears for longitudinal polarization in the photodissociation cross section (3.9).

For our calculations in section IV, we have to consider the more general case that the first interaction vertex occurs at z_a in the complex conjugated amplitude $M_{\text{fi}}^\dagger$, but at $z_b > z_a$ in the amplitude M_{fi}. This implies the further free evolution of (B5) from z_a to z_b,

$$I_L(\mathbf{b}_2 - \mathbf{b}_1|y_L, z_b)$$
$$= \int d^2\mathbf{b}_1'\,d^2\mathbf{b}_2'\,G_0(\mathbf{b}_2, z_b; \mathbf{b}_2', z_a|p_2)$$
$$\times I_L(\mathbf{b}_2' - \mathbf{b}_1'|y_L, z_a)\,G_0(\mathbf{b}_1', z_a; \mathbf{b}_1, z_b|p_1)$$
$$= \int d\mathbf{r}_b(z_a)\,K_0\left(\mathbf{r}_b(z_b), z_b; \mathbf{r}_b(z_a), z_a|\nu\alpha(1-\alpha)\right)$$
$$\times I_L(\mathbf{r}_b(z_a)|y_L, z_a)\,. \qquad \text{(B9)}$$

Here, we have used the notation introduced in equations (4.16) - (4.19) with $\mathbf{r}_b(z_a) = \mathbf{b}_2' - \mathbf{b}_1'$ and $\mathbf{r}_b(z_b) = \mathbf{b}_2 - \mathbf{b}_1$. Equation (B9) allows us to circumvent a notational problem which stems from the identity:

$$\int\limits_{-\infty}^{z_b} dy_L\,I(\Delta\mathbf{b}|y_L, z_b)$$
$$= e^{iq(z_b - z_a)}\int\limits_{-\infty}^{z_a} dy_L\,I(\Delta\mathbf{b}|y_L, z_a)\,. \qquad \text{(B10)}$$

Equation (B10) shows that if the points of first interaction differ in $M_{\text{fi}}^\dagger$ and M_{fi}, then phase factors $\exp(i\,q\,(z_b - z_a))$ arise in the squared free incoming wavefunction (B8). Hence, strictly speaking, we cannot do the y_L-integral *before* specifying the first points of interaction. Previous discussions of the q-$\bar q$-dipole do not have this difficulty, since they neglect these phase factors - a praxis which is justified for nuclear targets of size $L \ll 1/q$. If we want to keep the phases $\exp(i\,q\,(z_b - z_a))$ and yet write the photoabsorption cross section (3.9) in terms of Φ_L, we can use (B9) for a simple convention: whenever the free Green's function $K_0\left(\mathbf{r}_b(z_b), z_b; \mathbf{r}_b(z_a), z_a|\nu\alpha(1-\alpha)\right)$ acts on the first argument $\Delta\mathbf{b}$ of $\Phi_L(\Delta\mathbf{b};\Delta\bar{\mathbf{b}};\alpha)$, the result is a phase $\exp(i\,q\,(z_b - z_a))$, whenever it acts on the second argument, the result is the complex conjugated phase. This allows us to expand the cross section (4.23) in powers of the opacity without neglecting phase factors and without giving up the simple representation of $\sigma^{\gamma^* \to q\bar q}$ in terms of Φ.

We now turn to the transverse polarizations

$$\epsilon_\mu^\perp(\lambda) = \frac{1}{\sqrt{2}}\,(0, 1, i\lambda, 0)\,. \qquad \text{(B11)}$$

$$\Gamma_\lambda^T(\mathbf{y}) = \epsilon_\mu^\perp(\lambda)\Gamma^\mu$$
$$= \frac{-1}{2\sqrt{(1-\alpha)\alpha}}[\delta_{r,r'}i\nabla_\mathbf{y}\cdot\epsilon^\perp(\lambda)\,(r'(1-2\alpha)+\lambda)$$
$$+ \frac{m}{\sqrt{2}}\delta_{-r,r'}\,(1+\lambda r')]\,. \qquad \text{(B12)}$$

In contrast to the longitudinal case, this vertex does not factorize in the integrand of (3.7). However, the $\mathbf{y}$-integration can be done in analogy to (B6),

$$I_\lambda^\perp(\Delta\mathbf{b}|z_a)$$
$$= \int\limits_{-\infty}^{z_a} dy_L\,\int d^2\mathbf{y}_\perp\,e^{i\,q\,y_L - \epsilon\,|y_L|}\,G_0(\mathbf{b}_2; \mathbf{y}|p_2)$$
$$\times \Gamma_\lambda^T(\mathbf{y})G_0(\mathbf{y}; \mathbf{b}_1|p_1)$$
$$= \frac{(1-\alpha)\,\alpha\,\nu}{2\pi\,i}\,e^{i\,q\,z_a}\,2\,\Gamma_\lambda^T(\Delta\mathbf{b})\,K_0(\bar\epsilon\,|\Delta\mathbf{b}|)\,. \qquad \text{(B13)}$$

The squared transverse wavefunction reads then

$$\Phi_\perp(\Delta\mathbf{b};\Delta\bar{\mathbf{b}};\alpha) = \frac{\frac{1}{2}\sum_{\lambda,r,r'}I_\lambda^\perp(\Delta\mathbf{b}|z_a)\,I_\lambda^{\perp^*}(\Delta\bar{\mathbf{b}}|z_a)}{4\nu^2\alpha(1-\alpha)}$$
$$= \frac{\bar\epsilon^2}{2\,(2\pi)^2}\,\frac{\Delta\mathbf{b}\cdot\Delta\bar{\mathbf{b}}}{|\Delta\mathbf{b}|\,|\Delta\bar{\mathbf{b}}|}K_1(\bar\epsilon\Delta\mathbf{b})\,K_1(\bar\epsilon\Delta\bar{\mathbf{b}})\,\left(\alpha^2 + (1-\alpha)^2\right)$$
$$+ \frac{m^2}{2\,(2\pi)^2}\,K_0(\bar\epsilon\Delta\mathbf{b})\,K_0(\bar\epsilon\Delta\bar{\mathbf{b}})\,. \qquad \text{(B14)}$$

For the case that the points of first interaction z_a and z_b are different in the amplitude and complex conjugated amplitude, the convention explained below (B10) applies.

The arguments of the modified Bessel functions K_0 and K_1 in (B8) and (B14) specify the transverse separation of the q-$\bar q$ dipole pair. This separation is given approximately by $1/\bar\epsilon = 1/\sqrt{(1-\alpha)\alpha\,Q^2 + m^2}$. The higher the virtuality of the photon, the smaller the transverse size of this dipole. In general, the approximation of the virtual photon by the q-$\bar q$ Fock state is reasonable at sufficiently high virtuality, $Q^2 \gg 1$ GeV^2, above the vector meson dominance region [6]. There, the q-$\bar q$ separation is small enough to render the effects from string tension negligible and the quarks undergo independent scatterings. For a recent attempt to model interactions between the quarks, see Ref. [24].

APPENDIX C: CLASSIFICATION OF DIAGRAMS FOR (4.30)

In this appendix, we use the identities Fig. 7a and b to simplify the diagrammatic contributions to the inelastic part of the differential photoabsorption cross section (4.30). For each N-th order term in the opacity expansion of (4.30), we use the notational shorthand

$$\prod_{i=1}^{N} A_i^{n_i,m_i,o} . \qquad (C1)$$

Here, the index i labels the scattering potentials linked to the N-th order term, $i = 1$ being the first scattering potential. The superscripts n_i, m_i, o denote how the i-th scattering center is connected to the q-$\bar{q}$-system. Each scattering center is linked twice to the q-$\bar{q}$-system, once a momentum $\boldsymbol{\kappa}_\perp$ flows into the system, once it flows out. $n_i \in [1, 2]$ specifies whether the inflowing momentum is transfered to the upper quark line of momentum p_1 ($n_i = 1$) or the lower quark line of momentum p_2 ($n_i = 2$). Analogously, $m_i \in [1, 2]$ specifies whether the outflowing momentum comes from the upper ($m_i = 1$) or lower ($m_i = 2$) quark line. The remaining superscript $o \in [r, v, w]$ specifies the position of the two vertices from the i-th interaction w.r.t. the cut: either both vertices stand to the right of the cut ($o = v$) or to the left of the cut ($o = w$), or they are a real contribution ($o = r$) where one vertex stands to the right and the other to the left of the cut. We illustrate this notation with the examples in Fig. 12.

$$A_1^{11,r} A_2^{12,v} =$$
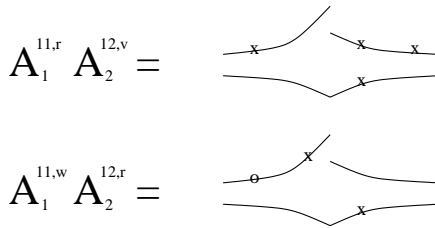
$$A_1^{11,w} A_2^{12,r} =$$

FIG. 12. Example of our notation (C1) for diagrammatic contributions to the photoabsorption cross section. For more details, see the text following (C1).

All N-th order contributions to the differential photoabsorption cross section (4.30) fall into exactly one of the following three classes:

1. There is at least one factor $A_j^{11,r}$ in the diagram (C1).

2. There is at least one factor $A_j^{12,r}$ or $A_j^{21,r}$ in the diagram (C1), but no factor $A_k^{11,r}$ (arbitrary k) and no factor $A_k^{22,r}$ with $k < j$.

3. (a) There is no factor $A_k^{11,r}$ (arbitrary k) but at least one factor $A_j^{12,r}$ or $A_j^{21,r}$ in the diagram (C1), and there is at least one factor $A_k^{22,r}$ with $k < j$.
   or
   (b) There are no factors $A_j^{11,r}$, $A_j^{12,r}$ or $A_j^{21,r}$ in the diagram (C1).

We now use the identities of Fig. 7a,b to show that many of the diagrams in these three classes cancel each other. In this way we determine the only remaining contribution for each of the three classes:

Class 1: The only non-vanishing contributions are those which contain no terms $A_l^{22,o}$, $A_l^{12,o}$ or $A_l^{21,o}$ with $o \in [r, v, w]$. They are shown in Fig. 10(a1).
Argument: Consider the subclass of diagrams containing factors $A_l^{22,o}$, $A_l^{12,o}$ or $A_l^{21,o}$. In case that there is more than one such factor in the diagram, consider the term with the largest index l, $l = k$ say. Leaving all terms $j \neq k$ unchanged, we find in this class of diagrams exactly one diagram with $A_k^{22,r}$, $A_k^{22,v}$ and $A_k^{22,w}$ on the k-th position. These three diagrams cancel each other due to the identity Fig. 7a. Also, for all terms $j \neq k$ unchanged, we find exactly one diagram with $A_k^{21,r}$ and $A_k^{21,v}$, which cancel due to the identity Fig. 7b. For the same reason, the two diagrams with $A_k^{12,r}$ and $A_k^{12,w}$ cancel each other (note that $A_k^{12,w} = A_k^{21,w}$ specifies the same k-th term in the same diagram). As a consequence, no contribution which contains terms $A_l^{22,o}$, $A_l^{12,o}$ or $A_l^{21,o}$ gives a non-vanishing contribution.

Class 2: The only non-vanishing contributions contain exactly one real term $A_j^{12,r}$ or $A_j^{21,r}$ with no real term $A_k^{11,r}$ or $A_k^{22,r}$, k arbitrary, and with no contact terms $A_k^{12,v}$, $A_k^{12,w}$, $A_k^{22,v}$, or $A_k^{22,w}$ for $k > j$. They are shown in Fig. 10(a2).
Argument: Choose in each diagram the term $A_j^{12,r}$ or $A_j^{21,r}$ with the lowest index j. Consider diagrams which contain terms $A_k^{22,o}$, $A_k^{12,o}$ or $A_k^{21,o}$, with $k > j$ and $o = r, v, w$. Taking k maximal and leaving all other terms unchanged, these diagrams cancel due to the identities Fig. 7a and b.

Class 3: The only non-vanishing contributions contain exactly one real term $A_j^{22,r}$ but no real terms $A_j^{11,r}$, $A_j^{12,r}$, or $A_j^{21,r}$ and no contact terms $A_k^{22,v}$, $A_k^{22,w}$, $A_k^{12,v}$ or $A_k^{12,w}$ with $k > j$. They are shown in Fig. 10(a3).
Argument: Consider in each diagram the term $A_j^{22,r}$ with lowest index j. Look then at the largest index $k > j$ linking to the p_2-line. Leaving all other terms unchanged, the sum of the contributions with different configuration at position k ensures cancellation: $A_k^{22,r}$, $A_k^{22,v}$ and $A_k^{22,w}$ cancel each other due to identity Fig. 7a. $A_k^{21,r}$, $A_k^{21,v}$ and $A_k^{12,r}$, $A_k^{21,w}$ cancel each other due to identity Fig. 7b. Thus only contributions with exactly one real term $A_j^{22,r}$ survive cancellation.

[1] G.T. Bodwin, S.J. Brodsky and G.P. Lepage, Phys. Rev. **D39** (1989) 3287.
[2] S.J. Brodsky, A. Hebecker and E. Quack, Phys. Rev. **D55** (1997) 2584.
[3] A.H. Mueller and J. Qiu, Nucl. Phys. **B268** (1986) 427.
[4] A.H. Mueller, Nucl. Phys. **B335** (1990) 115.
[5] N.N. Nikolaev and B.G. Zakharov, Z. Phys. **C49** (1991)

607.

[6] G. Piller and W. Weise, hep-ph/9908230.

[7] A.H. Mueller, Nucl. Phys. **B558** (1999) 285-303.

[8] Y.V. Kovchegov and L. McLerran, Phys. Rev. **D60** (1999) 054025.

[9] M. Luo, J.W. Qiu, and G. Sterman, Phys. Rev. **D49** (1994) 4493 and Phys. Rev. **D50** (1994) 1951.

[10] X. Guo, Phys. Rev. **D58** (1998) 036001 and 114033.

[11] R.J. Fries, A. Schäfer, E. Stein and B. Müller, Phys. Rev. Lett. **83** (1999) 4261 and hep-ph/0002074.

[12] M. Gyulassy and X.-N. Wang, Nucl. Phys. **B420** (1994) 583.

[13] X.-N. Wang, M. Gyulassy and M. Plümer, Phys. Rev. **D51** (1995) 3436.

[14] B.G. Zakharov, JETP Letters **63** (1996) 952, **65** (1997) 615.

[15] R. Baier, Y.L. Dokshitzer, A.H. Mueller, S. Peigné and D. Schiff, Nucl. Phys. **B483** (1997) 291.

[16] R. Baier, Y.L. Dokshitzer, A.H. Mueller, S. Peigné and D. Schiff, Nucl. Phys. **B484** (1997) 265.

[17] R. Baier, Y.L. Dokshitzer, A.H. Mueller and D. Schiff, Phys. Rev. **C58** (1998) 1706.

[18] R. Baier, Y.L. Dokshitzer, A.H. Mueller and D. Schiff, Nucl. Phys. **B531** (1998) 403.

[19] B.G. Zakharov, Phys. Atom. Nucl. **61** (1998) 838 [Yad. Fiz. **61** (1998) 924], hep-ph/9807540.

[20] B.Z. Kopeliovich, A. Schäfer and A.V. Tarasov, Phys. Rev. **C59** (1999) 1609.

[21] U.A. Wiedemann and M. Gyulassy, Nucl. Phys. **B560** (1999) 345-382.

[22] R. Baier, Y.L. Dokshitzer, A.H. Mueller and D. Schiff, Phys. Rev. **C60** (1999) 064902.

[23] M. Gyulassy, P. Levai and I. Vitev, hep-ph/9907461.

[24] B.Z. Kopeliovich, A. Schäfer and A.V. Tarasov, hep-ph/9908245.

[25] O. Nachtmann, Ann. Phys. (N.Y.) **209** (1991) 436.

[26] R. Baier, Y.L. Dokshitzer, A.H. Mueller, S. Peigné and D. Schiff, Nucl. Phys. **B478** (1996) 577.

[27] Y.V. Kovchegov and A.H. Mueller, Nucl. Phys. **B529** (1998) 451.

[28] W. Buchmüller and A. Hebecker, Nucl.Phys. **B476** (1996) 203.

[29] P. Hoyer and S. Peigné, Phys. Rev. **D57** (1998) 1864 and Phys. Rev. **D59** (1999) 034011.

[30] R.D. Field, *Applications of Perturbative QCD*, Addison-Wesley, 1989.

[31] B.G. Zakharov, Sov. J. Nucl. Phys. **46** (1987) 922.

[32] W. Buchmüller, T. Gehrmann and A. Hebecker, Nucl. Phys. **B537** (1999) 477.

[33] N.H. Christ, Phys. Rev. Lett. **34** (1975) 355.

[34] I.Ya. Aref'eva, Theor. Math. Phys. **43** (1980) 353.

[35] P.M. Fishbane, S. Gasiorowicz and P. Kaus, Phys. Rev. **D24** (1981) 2324.

[36] H.G. Dosch and Yu.A. Simonov, Phys. Lett. **B205** (1988) 339.

[37] H.G. Dosch, E. Ferreira and A. Krämer, Phys. Rev. **D50** (1994) 1992.

[38] M. Gyulassy, P. Levai and I. Vitev, work in preparation.